NTNU

Norwegian University of
Science and Technology

Nonlinear Model Predictive Pressure Control during Drilling Operations

Øyvind Breyholtz

Master of Science in Engineering Cybernetics
Submission date: June 2008
Supervisor: Ole Morten Aamo, ITK

Norwegian University of Science and Technology
Department of Engineering Cybernetics

Problem Description

Improved pressure control during drilling may lead to: the posibility to drill wells that previously has been considered to be undrillable, reduced pressure related drilling problems and resulting rig non-productive time, reduced formation damage which may lead to reduced production, and increased safety for drilling crew and evironement by reducing the posibility for a kick or a blow-out. The objective of this thesis is to design a controller which improves the pressure control during drilling. During drilling operations the bottomhole pressure variations should be kept less than 2.5 bars.
Topics that should be addressed are:
1) Literature review of:

- Managed pressure drilling
- Nonlinear Model Predictive Control

2) Implement an observer for the bottomhole pressure

3) Implement nonlinear model predictive pressure control by using StatoilHydro's MPC tool, SEPTIC.

4) Analyze the performance of the controller

Assignment given: 07. January 2008
Supervisor: Ole Morten Aamo, ITK

Summary

Drilling into mature, depleted fields is often difficult because of tight pressure margins. Increasing the pressure control will enable wells that previously were considered undrillable, to be drilled. Enabling drilling and increased oil recovery from depleted fields would most likely lead to a substantial increase in profit margains. A better pressure control will also increase the safety of the drilling crew, because the risk of unwanted situations such as a kick or a blow-out is decreased, also reducing the risk of unwanted environmental influence, e.g. oil spill.

To compensate for the lack of a continuous measurement of the bottomhole pressure during drilling operations, an adpative observer of the bottomhole pressure is implemented. The observer implemented is tested, and shows promising results in estimating both the bottomhole pressure and the friction coefficient in the well during a pipe connection procedure.

To control the pressure in the well, a low-order nonlinear model predicitve controller is developed, and it has been tested to perform well during the pipe connection procedure, where it maintains the pressure within the predefined boundaries. In this thesis both the obsever and the controller will be tested against an artificial well; simulated by a commercial software.

Preface

This master thesis was written in my 10th and final semester for the degree of Master of Technology at the Department of Engineering Cybernetics, Faculty of Information Technology, Mathematics and Electrical Engineering at the Norwegian University of Science and Technology. The work and this report was written in the period from january to june 2008. The assignement has been carried out under the supervision of Professor Ole Morten Aamo and co-supervision of Dr. John-Morten Godhavn at StatoilHydro's research center at Rotvoll, Trondheim.

StatoilHydro has been involved in the project formulation, and have provided workspace at their facilities with full acsess to their software utilities. I would like to thank Professor Ole Morten Aamo for assigning this project to me, and for his role as supervisor. I would especially like to thank Dr. John-Morten Godhavn for helping me out on a daily basis, and for patiently answering all my questions. There are several people at StatoilHydro's research center that have been of great assistance to me. Dr. Stig Strand and Morten Fredriksen have been an invaluable help when implementing the model predicitve controller. I would also like to thank Håvard Torpe for support with SEPTIC.

I would also like to thank Dr. Gerhard Nygaard at the International Research Institute of Stavanger for providing me with a dynamic well simulator, and for helping we with problems I have encountered when using it.

Finally I would like to thank Øivind Stamnes for his help when implementing the observer of the bottomhole pressure, and Jørn, Jalal and Marthe, whith whom I have been sharing office this semester, for their support.

Contents

List of Figures

List of Tables

Abbreviations

CVs	Controlled variables
DMC	Dynamic Matrix Control
DVs	Disturbance Variables
FIR	Finite Impulse Respons
IDCOM	Identification and Control
IRIS	International Research Institute of Stavanger
LQG	Linear Quadratic Gaussian
MPC	Model Predictive Control
MPD	Manage Pressure Drilling
MPHC	Model Predictive Heuristic Control
MPT	Mud Pulse Telemetry
MVs	Manipulated Variables
NMPC	Nonlinear Predictive Control
NP	Nonlinear Programming
QDMC	Quadratic Dynamic Matrix Control
QP	Quadratic Programming
RHC	Receding Horizon Control
SISO	Singel Input Singel Output
SEPTIC	Statoil's Estimation and Prediction Tool for Identification and Control

Chapter 1

Motivation

1.1 Pore, Fracture and Collapse Pressure

All formations are porous to some degree, and these pores contain either water, gas or oil, or any combination of these fluids. The pressure exerted by the fluids within these pores are often refered to as pore pressure, or in case of a gas or oil reservoir, reservoir pressure. The formation pressures must be less then the total overburden pressure (The overburden pressure is the pressure exercised by the weight of fluids and formation materials which lie above any particular depth point). If not, the fluid would flow through the overlying formations, and escape until the pressure difference equalizes. A normal formation pressure is defined to be equal to the hydrostatic pressure exerted by all the fluids in formations above. In some cases, e.g. an artesian well, the formation pressure may be abnormally high. A basic introduction to formation pressure can be found in [Skalle, 2005]. The pore pressure will be denoted p_{res} from now on.

The fracture pressure is the pressure which will cause the rock formation to fracture hydraulically. The fracture pressure will be denoted p_{frac} from now on.

Collapse pressure is the pressure at which the well will catastrophically deform as a result of differential pressure acting from the surrounding formations to the well. The collapse pressure of a perfect round tubing is relatively high, but even slightly ovality will significantly reduce the differential pressure at which the well collapses. The collapse pressure will be denoted p_{coll} from now on.

The relationship between the three pressures mentioned above is

$$p_{coll}(t,x) < p_{res}(t,x) < p_{frac}(t,x) \tag{1.1}$$

where t is the time, and x is the vertical position in the well.

1.2 Pressure Control

During drilling operations the pressures mentioned above must be taken into consideration. The success of the hole drilling operation will be dependent up on managing the pressure in the well. If the fracture and collapse pressure is first taken into consideration, it is important that the pressure in the well is kept within these pressures (illustrated in figure 1.1).

$$p_{coll}(t,x) < p_{well}(t,x) < p_{frac}(t,x) \tag{1.2}$$

If the pressure in the well is not kept within these boundaries, there will be unwanted consequences. The case of exceeding the fracture pressure is first considered.

$$p_{coll}(t,x) < p_{frac}(t,x) < p_{well}(t,x) \tag{1.3}$$

Exceeding the fracture pressure will fracture the rock formation, and there is a high risk of an underground blowout. [Grace, 1994] defines an underground blowout as the flow of formation fluids from one zone to another. The underground blowout can usually be detected by a lack of pressure response on the annulus while pumping on the drillpipe. It can be very difficult to handle, and can result in a dangerous and destructive situation. If the underground blowout is within 3000- 4000 feet from the surface, it is possible for the flow to fracture to the surface outside the casing. If the drilling is performed offshore, it is most likely that the crater will occur immediatly below the rig. If the crater is below the rig or platform, the entire installation can be lost, with severe consequences.

The opposite situation; a pressure drop in the well beneath the collapse pressure:

$$p_{well}(t,x) < p_{coll}(t,x) < p_{frac}(t,x) \tag{1.4}$$

If the pressure in the well is lower then the collapse pressure, it can lead to an unstable hole, where the walls falls onto the drillpipe. This can lead to a stuck pipe, or a twist-off, which is breaking the drillpipe. If the drillpipe is twisted off, the well probably has to be drilled again.

The reservoir pressure must of course also be taken into consideration, and will significantly impact the drilling operations. Ordinary drilling operations are usually performed with a higher hydrostatic pressure than formation pressure, also known as overbalanced conditions.

$$p_{coll}(t,x) < p_{res}(t,x) < p_{well}(t,x) < p_{frac}(t,x) \tag{1.5}$$

The result of this difference is an influx of fluids and solids into the formation. Usually, the volume of invading fluids is small and the invasion is limited to

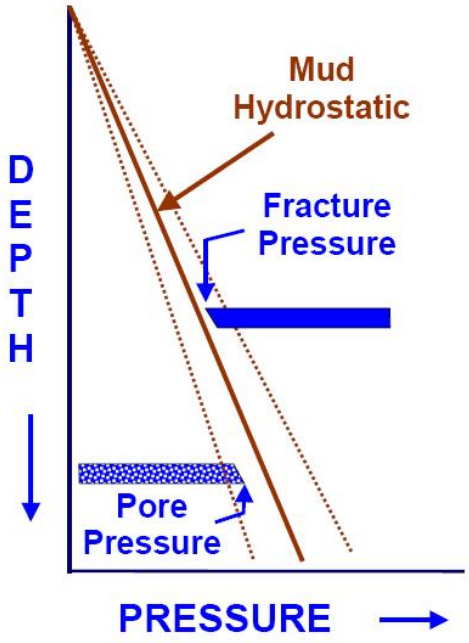

Figure 1.1: Hydrostatic Pressure

a short distance from the wellbore. The depth of solids invasion is less than the fluid invasion, but results in more severe formation damage.Golan and Whitson [1986]

If the well pressure unintentionly drops below the reservoir pore pressure, there will be an influx from the reservoir to the well.

$$p_{coll}(t,x) < p_{well}(t,x) < p_{res}(t,x) < p_{frac}(t,x) \tag{1.6}$$

If this flow is small, there will be a change in the density of the mud, which is measured at the surface, and the drilling fluid is said to be 'gas cut', 'salt water cut' or 'oil cut'.Skalle [2005]. If this influx from the reservoir is large, it is known as a kick or if the influx is uncontrolled, a blow-out, which is a more serious and dangerous situation. A kick must be handled when it occurs, and blowout prevention equipment is needed to close the well. If gas migrates from the reservoir to the well, it is more possible that a kick occurs, than if the fluid is oil or water. Grace [1994] lists the following key reasons for a pressure drop, which may result in a kick:

- Mud weight less than formation pore pressure
- Failure to keep the hole full while tripping

- Swabbing while tripping
- Lost circulation
- Mud cut by gas, water or oil

A kick can sometimes by hard to detect, but there are some signs that a kick has occured. Grace [1994] lists the following indications:

1. Sudden increase in drilling rate
2. Increase in fluid volume at the surface, which is commonly termed a pit level increase or an increase in flow rate
3. Change in pump pressure
4. Reduction in drillpipe weight
5. Gas, oil, or water-cut mud

The first indication of a kick, is a sudden increase in drillrate, known as a 'drilling brake'. The increase in drillrate is an indication of penetration of a porous formation. The next warning sign is an increase in flow rate caused by the influx of formation fluids. The influx may be rapid or virtually unnoticeable, depending on the formation productivity. Changes in flow rate or pit level should never be ignored. The influx from the reservoir will decrease the hydrostatic pressure in the well. This would be observed by a reduction in the pump pressure.

The desire to maintain the pressure within these limitations, rises the need for accurate control of the pressure gradient in the well. A technic used to control the pressure in the well is Managed Pressure Drilling (MPD). An introduction to MPD, and a describtion of different MPD solutions can be found described in Hannegan [2006].Definition of MPD by IADC's MPD Subcommittee:

> *'An adaptive drilling process used to precisely control the annular pressure profile throughout the wellbore. The objectives are to ascertain the downhole pressure environment limits and manage the hydraulic pressure profile accordingly'.*

MPD consist of different solution for better control of the pressure gradient in the well. A better control of the pressure gradient will lead to the possibility of drilling wells, that has been considered to be undrillable. MPD techniques can therefore be used to increase the oil recovery from depleted and mature

reservoirs. However, controlling the pressure gradient is complicated by the absence of a continuous measurement of the pressure gradient in the well. The measurement of the pressure is sent to the surface by a mud pulse telemetry (MPT) system. This system has a low bit rate, and are therefore unsuited for control purposes. The desire to control the pressure in the well rise the need to estimate the pressure gradient in the well.

Several articles and reports on MPD has been written. The reader may refer to Nygaard and Nævdal [2006] and Nygaard et al. [2007] for a control solution with an NMPC control scheme, or Rognmo [2007] for a H_∞ control scheme.

1.3 Drilling Mud

Drilling mud was introduced with rotary drilling in 1900, and it's main function was to remove the cuttings from the well. With time, drilling has become more sophisticated, and the functions of the mud has increased to include several other factors. Moore [1986] defines the primary functions of the mud as following:

- Lifts formation cuttings to the surface
- Controls subsurface pressures
- Lubricates the drillstring
- Cleans the bottom of the hole
- Aids in formation evaluation
- Protects formation productivity
- Aids formation stability

The mud has evolved from beeing a simple fluid to become a complex mixture of liquids, solids and chemicals. The reader may refer to Moore [1986] for a general introduction to the functions and composition of drilling fluids. The discussion in this section will give a brief summary of the information presented in Moore [1986].

Lifting formation cuttings is an essential function of the mud. If the specific gravity of the cuttings are higher then the mud, the cuttings will slip downwards in the mud. While the flow in the annulus is viscous or laminar, the slip velocity of the cuttings are directly related to the thickness or shear

characteristics of the mud. Sometimes the decision to increase the mud thickness/weight will affect other aspects of the drilling. The hydrostatic pressure, and the circulating pressure losses will increase. **Bottomhole Cleaning** is generally improved by having thin fluids flow at high shear rates through the bit. If they have good shear characteristics, viscous fluids can be good for bottomhole cleaning.

Selecting the specific weight of the mud to **control subsurface pressures** introduces several problems. As the mud weight decreases, the drilling rate will increase, and lost circulation problems are minimized. (burde skrive hva lost-circulation problemer er)

Lubrication and cooling of the drillstring is an important function of the mud. Adequate cooling may prolong the expected lifetime of the equipment, and reduce hole problems, such as torque, drag, and differential pressure sticking. Lubricants include betonite, oil, detergents, graphite, asphalts, special surfactants, and walnut hulls.

An increase in **formation evaluation** requirements has affected the drilling fluids significantly. Viscosity has been increased to improve the removal of cuttings, special mud has been developed to improve logging characteristics.

Protection of formation productivity is one of the most important aspects of drilling, since noncommerical hydrocarbons zones often are due to formation damage through invason of mud or filtrate.

Economides et al. [1998] choose to group drilling fluids into four basic types:

- Water-based muds
- Oil-based muds
- Synthetic-based muds
- Pneumatic drilling fluids

Water based muds make up the majority of drilling fluids. The water can be either fresh or salt water. Fresh water is the base of must muds, and has an advantage in beeing generally accessible and cheap. It is easy to control, even when it is loaded with solids. Salt water has also become more commen as a base, because of it's accessibility in offshore operations. There are many disadvantages using salt water. It reduces the effectivness of formation evaluation methods, corrosion problems are increased, and mud costs are increased. Oil has been used as a base almost as long as water. Initally it was used to protect potential productive formations. Oil-based muds are highly

inhibitive, resistant to contaminants, stable at high temperatures and pressures, highly lubricious, noncorrosive, and flexible [Economides et al., 1998]. Resulting in reduced torque, drag, and pipesticking problems. Synthetic-based mud represents the latest technology, and provides high performance, comparable to the performance of oil-based mud, without the objectionable toxicity and environmental impact. [Azar and Samuel, 2007] lists the following different pneumatic fluids: *Dry air*, *Mist*, *Foam*, and *Gasified mud*. Pneumatic fluids are normally used in special applications to minimize damage to productive formations, prevent loss of circulation, and achieve very high penetration rates. There are some drawbacks to pneumatic fluids. Even though they adequatly handle normal drilling fluids, there are problems with cuttings suspension and filter cake deposistion. Moore [1986] lists the following disadvantages to using oil-based mud compared with water-based mud.

- Oil costs more than water
- Environmental pollution problems are increased
- Drilling crews generally do not like to work around oil
- Annular circulatating pressures may be higher with oil-based muds
- Gas kicks are more difficult to control because of the solubility of gas in oil

One last important point is that oil-based mud is compressed under pressure; increased pressure leads to a higher fluid density. Pressure changes has almost no effect on water-based mud.

1.4 Scope and outline of thesis

The scope of this thesis has been to develop a nonlinear model predictive controller (NMPC). The controller is to be tested on a pipe connection scenario. The NMPC scheme will be based up on a low-order singel phase model of the well. An observer of the bottomhole pressure (BHP) will be implemented to estimate the pressure in the well. To simplify the problem, only the BHP will be considered, and the pressure gradient in the rest of the well will be ignored.

- In chapter 2 a low order model of the well is derived.
- Chapter 3 presents an adaptive observer for the bottomhole pressure.
- Chapter 4 gives a brief historical introduction to NMPC, and continuous with a more detailed discussion around concept of NMPC. The end of the chapter describes the implementation of the NMPC scheme.
- In chapter 5 some important results are presented.
- Chapter 6 concludes the report, and future work is discussed.

Chapter 2

Modeling

As stated previously, there will not exsist a continuous measurment of the BHP, and there is a need of an observer to estimate the pressure. The observer which will be presented in chapter 3, needs a model of the dynamics in the well. The model predictive controller (MPC) presented in chapter 4 also needs a model to predict future responses of the system. The basic fluid mechanics presented in this chapter is mainly from [White, 2003]. The more specific well model is orginally developed in an unpublished internal document by [Kaasa]. It can also be found in a master thesis [Øyvind Nistad Stamnes, 2007]. The model presented is a simplified model, which only considers a singel phase flow of drilling fluids. Reservoir influx will not be taken into consideration. A similar two phase model can be found in [Nygaard and Nævdal, 2006].

The well model, described in figure 2.1, consists of a jointed drillpipe, two mud pumps, a topside choke and a drill bit. The drillpipe consists of segments 100 feet long, joined together, with the drill bit at the end. At the topside the main mud pump is connected to the drill pipe, and the drilling fluids flow through the drillpipe and the bit. It then flows up the annulus, bringing cuttings to the surface. At the surface the mud flows through the topside choke, before the cuttings are removed from the mud, and the mud is reused. The second mud pump is not connected to the drill pipe, but directly to the annulus. It can be used to increase the pressure in the well, and to maintain a degree of circulation during a pipe connection. For modelling purposes the well will be divided into two different control volumes as shown in figure 2.1.

In the model which is derived later in this chapter, all temperature effects are neglected, even though the temperature variations in the well can be significant. The temperature in the well is assumed to be constant(isothermal conditions). The modelling will be based on the equation of continuity (mass

conservation), the equation of momentum (Navier-Stokes) and the equation of state. Since all temperature effects are neglected, the equation of energy will not be further discussed.

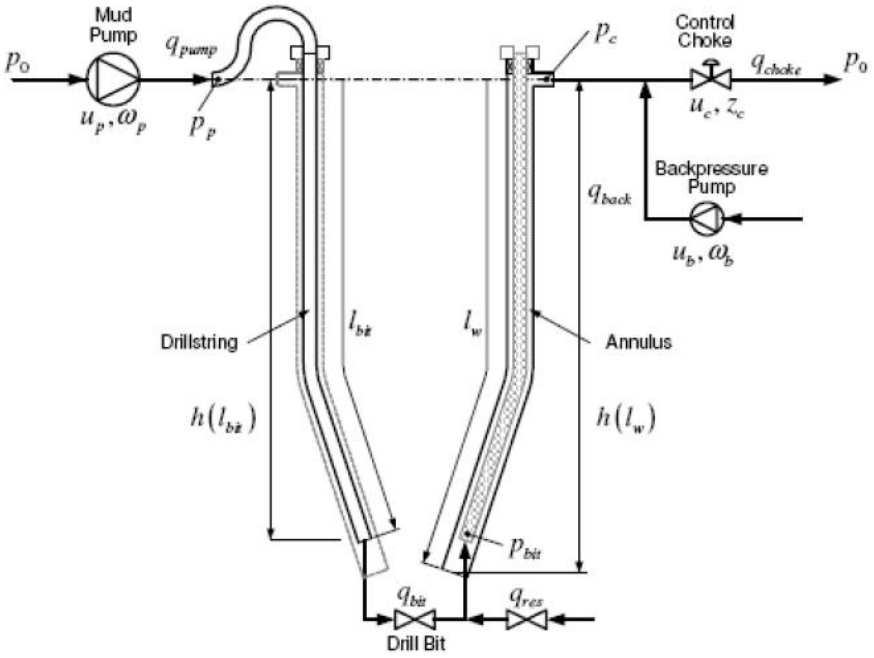

Figure 2.1: Well divided into two control volumes. [Kaasa]

2.1 Equation of State

The drilling mud will have a density which will change as a function of pressure and temperature. The changes of fluid density are small for a liquid, and the linearized function will be used as an approximation.

$$\rho = \rho_0 + \frac{\partial \rho}{\partial p}(p - p_0) + \frac{\partial \rho}{\partial T}(T - T_0) \tag{2.1}$$

p_0,ρ_0 and T_0 is a set of conditions, which equation 2.1 is linearized around[Kaasa]. While the energy equation will not be taken into consideration, and isothermal conditions are assumed, the equation simplifies into

$$\rho = \rho_0 + \frac{\partial \rho}{\partial p}(p - p_0) \tag{2.2}$$

It is normal to define the bulk modulus of a liquid. The bulk modulus is a term used to describe the compressibilty of a fluid[White, 2003].

$$\beta = -V\frac{\partial p}{\partial V} = \rho\frac{\partial p}{\partial \rho} \tag{2.3}$$

The bulk modulus is related to the speed of sound

$$c = \sqrt{\frac{\partial p}{\partial \rho}} = \sqrt{\frac{\beta}{\rho}} \tag{2.4}$$

where c denotes the speed of sound. The bulk modulus can also be described by the differential form [Egeland and Gravdahl, 2002]

$$\frac{\partial \rho}{\rho} = \frac{\partial p}{\beta} \tag{2.5}$$

The bulk modulus is inserted into equation 2.2, and the final linear approximation of the density is found.

$$\rho = \rho_0 + \frac{\rho_0}{\beta}(p - p_0) \tag{2.6}$$

As stated in section 1.3, there is a significant difference in the bulk modulus for oil-based and water-based mud. If the mud is oil-based, the hydrostatic pressure in the well will increase nonlinear with increasing depth. This phenomenon should be taken into consideration, and the approximation in equation 2.6 should not be ignored.

2.2 Friction

Friction can not be ignored in a viscous flow. The friction terms that will be discussed in this section is head losses and minor losses.

2.2.1 Head losses

Head losses (or Major losses) is a term used to describe the losses in sections consisting of straight pipes. The friction loss term, can be given by

$$\frac{\partial F}{\partial x} = S(x)\frac{\partial}{\partial x}(\sigma_w) \tag{2.7}$$

where σ_w is the wall shear stress. For a pipe flow, the friction term can be determined by

$$\sigma_w = f\frac{1}{4}\frac{\rho}{2}v^2 \tag{2.8}$$

The parameter f is dimensionless, and is called the Darcy friction factor, after Henry Darcy, which first established the effect of roughness on pipe resistance. The friction factor for smooth pipes is usually asummed to be

$$f = 0.316 \ \mathrm{Re}^{-\frac{1}{4}} \tag{2.9}$$

This relationship applies to Reynolds numbers less than 10^5. Since the drilling mud is a compressible fluid, the estimate may be very crude.

2.2.2 Minor Losses

Most pipe systems consist of more then straight pipes. Bends, valves and tees add to the overall head loss of the system. These losses are generally refered to as minor losses[Munson et al., 1998]. The term minor loss does not indicate a small and unsignificant loss. In the case of incompressible flow, the pressure drop will be equal to:

$$\Delta p = K_L \frac{1}{2} \rho V^2 \tag{2.10}$$

Where K_L is an empirical loss coefficient:

$$K_L = \frac{\Delta p}{\frac{1}{2}\rho V^2} \tag{2.11}$$

The value of K_L will be strongly dependent on the Reynolds number, and the geometry of the component. The Reynolds number of the pipe is $Re = \frac{\rho V D}{\mu}$.

2.2.3 Orifice Flow

The head loss assosicated with a valve is a common minor loss, and the size of the loss may be a significant portion of the resistance in the system. The area of the valve is much smaller than the upstream area. The velocity of the flow is given in the equation

$$v = C_d \sqrt{\frac{2(p_1 - p_0)}{\rho}} \tag{2.12}$$

where C_d is the discharge coefficient. The discharge coefficient accounts for an additional flow concentration know as *vena contracta*. Inserting $v = \frac{Q}{A}$, gives an expression of the volume flow.

$$q = C_d A(x) \sqrt{\frac{2(p_1 - p_0)}{\rho}} \tag{2.13}$$

This equation is based on the assumption of a steady and icompressible flow, which is not valid for our system. However, this approximation is used.

2.2.4 Friction Gradient

The pressure loss due to friction will be the sum of the minor losses and the head losses. As stated in equation (2.7)- (2.8), the friction loss in the pipeline will be

$$\frac{\partial F}{\partial x} = S(x)\frac{1}{4}f\frac{\rho}{2}v^2 \tag{2.14}$$

The minor losses can be related to the friction gradient according to

$$\frac{\partial F}{\partial x} = A(x)\frac{\partial K}{\partial x}\frac{\rho}{2}v^2 \tag{2.15}$$

where K is the loss coefficient over a length ΔL, and the minor loss gradient is

$$\frac{\partial K}{\partial x} = \frac{K}{\Delta L} \tag{2.16}$$

The total friction gradient of the well will be the sum of the minor and major losses.

$$\frac{\partial F_F}{\partial x} = \frac{1}{4}fS(x)\frac{\rho}{2}\left(\frac{q}{A(x)}\right)^2 + \frac{\partial K}{\partial x}A(x)\frac{\rho}{2}\left(\frac{q}{A(x)}\right)^2 \tag{2.17}$$

where A(x) and S(x) are the cross sectional area and perimeter of the flow.

2.3 Equation of Continuity

The derivation in this chapter starts with the one-dimensional continuity equation. The derivation of the continuity equation can be found in appendix B.

$$\frac{\partial \rho}{\partial t} + \frac{\partial}{\partial x}(\rho u) = 0 \tag{2.18}$$

As described in [Kaasa] the continuity function is integrated over a deformable control volume, with lenght equal to L

$$\frac{d}{dt}\left(\int_0^L \rho A(x)dx\right) = \sum m_{in} - \sum m_{out} \tag{2.19}$$

where

$$m = \int_0^L \bar{\rho}(p)A(x)dx = \rho(\bar{p})V \tag{2.20}$$

V is the total volume in the well, and $A(x)$ is the area in the well. Equation 2.19 is rewritten on the form

$$\dot{m} = \sum m_{in} - \sum m_{out} \tag{2.21}$$

The density in the well will not be constant, but will be approximated by an average density, which will be dependent on pressure variations in the well.

$$\bar{\rho}(p) = \frac{1}{V}\int_0^L \rho(x,p)A(x)dx \tag{2.22}$$

The left part of equation 2.21 can be expressed as

$$\dot{m} = \frac{\partial m}{\partial t} = \frac{\partial \bar{\rho}(p)V}{\partial t} = V\frac{\partial \bar{\rho}(p)}{\partial t} + \bar{\rho}(p)\frac{\partial V}{\partial t} \tag{2.23}$$

Insert the bulk modus into equation 2.23

$$\dot{m} = \bar{\rho}(p)\frac{V}{\beta}\frac{\partial p}{\partial t} + \bar{\rho}(p)\frac{\partial V}{\partial t} = \rho(\frac{V}{\beta}\dot{\bar{p}} + \dot{V}) \tag{2.24}$$

This expression is inserted into equation 2.21

$$\bar{\rho}(p)(\frac{V}{\beta}\dot{\bar{p}} + \dot{V}) = \sum m_{in} - \sum m_{out} \tag{2.25}$$

Rearranging the equation gives

$$\frac{V}{\beta}\dot{\bar{p}} + \dot{V} = \frac{1}{\bar{\rho}(p)}(\sum m_{in} - \sum m_{out}) \tag{2.26}$$

The assumption of $\frac{1}{\bar{\rho}(p)}\sum m_{in} = \sum q_{in}$ and $\frac{1}{\bar{\rho}(p)}\sum m_{out} = \sum q_{out}$ is made. Resulting in

$$\frac{V}{\beta}\dot{\bar{p}} + \dot{V} = (\sum q_{in} - \sum q_{out}) \tag{2.27}$$

This result will be used on the well in figure 2.1. The well will be considered as two seperate subsystems(two different control volumes). The first subsystem will consist of the drillpipe-section of the well. (The left part of figure 2.1) At the topside the drilling fluids will be pumped into the drillpipe. The mud pump will have a pressure of p_p. The drillpipe will have a length of l_d, an inner and outer radius of r_{di} and r_{do}, and volume of V_d. The volume of the drillpipe will change accordingly to different well operations. During surge and swab operations (insertion and extraction off the drillpipe) the volume will change. The boundary of this subsystem will be the drill bit. The fluids

that pour out of the bit, will be denoted q_{bit}. This is inserted into equation 2.27 and the resulting differential equation for the subsystem forms:

$$\frac{V_D}{\beta}\dot{p}_p = q_{in} - q_{bit} - \dot{V}_D \tag{2.28}$$

The remaining part of the system will be considered in the second system. The connection between the to subsystems will be the flow through the bit. For the second subsystem, the inflow to the control volume will be the flow through the bit, a possible influx from the reservoir, and the flow from the backpressure pump. The outlet of the annulus subsystem is the flow through the topside choke. The annulus will have a length of l_a, a volume of V_a, and a radius of r_a.

$$\frac{V_A}{\beta}\dot{p}_c = q_{bit} + q_{res} + q_{bp} - q_{out} - \dot{V}_A \tag{2.29}$$

2.4 Equation of Motion

Using Newton's second law of motion and the assumption of one dimensional flow, the momentum balance is obtained. The derivation of this equation can be found in appendix C.

$$\sum F = \frac{\partial}{\partial t}(\int_{CV} V_s \rho \text{ dV}) + \sum (\dot{m}V_s)_{out} + \sum (\dot{m}V_s)_{in} \tag{2.30}$$

The sum of the forces acting on the fluid will consist of two different type of forces, body forces and surface forces.

$$\sum F = F_{surface} + F_{gravity} \tag{2.31}$$

The body force that will be taken into consideration in this system, is gravity. The size of the component of the gravity force that acts on the body, will depend up on the angel between the streamline and the gravity force [Munson et al., 1998]. In this particular case having done the assumption of a one dimensional vertical flow, the streamline will be parallell with the gravity force, as illustrated in the right part of figure 2.2.

$$F_{gravity} = \rho g sin\theta = \rho g \frac{\partial h}{\partial x} \tag{2.32}$$

The second type of forces that will be considered, are the surface forces. The viscous stresses on the surfaces of the control volume lead to surface forces. These surfaces forces are the sum of the hydrostatic pressure, and friction forces (viscous stress) due to motion.[White, 2003]

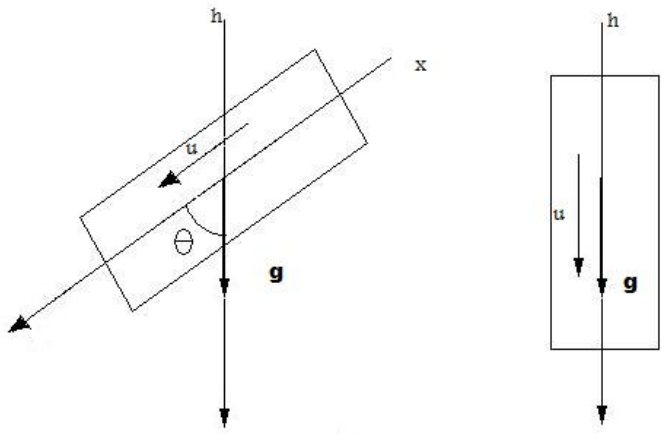

Figure 2.2: Body Force

$$F_{surface} = -\frac{\partial p}{\partial x}Adx - \frac{\partial F_F}{\partial x}dx \tag{2.33}$$

Inserting equation 2.32 and 2.33 into equation C.6:

$$\rho\frac{dV_s}{dt}A(x)dx = -\frac{\partial p}{\partial x}A(x)dx - \frac{\partial F_F}{\partial x}dx + \rho g\frac{\partial h}{\partial x}A(x)dx \tag{2.34}$$

$$\rho\frac{dV_s}{dt}dx = -\partial p - \frac{1}{A(x)}\frac{\partial F_F}{\partial x}dx + \rho g\partial h \tag{2.35}$$

This is a reduced form of a well-known equation, Navier-Stokes. The equation is reduced from full order to one-dimensional flow. Due to the assumption of one-dimensional flow: $V_s = \frac{dx}{dt}$. The differential equation is integrated over a control volume with length L.

$$\int_0^l \frac{\rho}{A(x)}dx\frac{dq}{dt} = -\int_{p(0)}^{p(l)}\partial p - \int_0^l \frac{1}{A(x)}\frac{\partial F_F}{\partial x}dx + \int_{h(0)}^{h(l)}\rho g\partial h \tag{2.36}$$

$$\int_0^l \frac{\rho}{A(x)}dx\frac{dq}{dt} = p(0) - p(l) - \int_0^l \frac{1}{A(x)}\frac{\partial F_F}{\partial x}dx + \rho g\left[h(l) - h(0)\right] \tag{2.37}$$

The expression $\frac{\partial F_F}{\partial x}$, described in equation 2.17 is inserted into the equation.

$$\int_0^l \frac{\rho}{A(x)} dx \frac{dq}{dt} = p(0) - p(l) - \int_0^l \frac{1}{A(x)} \frac{1}{4} f S(x) \frac{\rho}{2} \left(\frac{q}{A(x)(x)} \right)^2 \tag{2.38}$$

$$+ \frac{\partial K}{\partial x} A(x) \frac{\rho}{2} \left(\frac{q}{A(x)} \right)^2 dx + \rho g \left[h(l) - h(0) \right] \tag{2.39}$$

Equation 2.38 can be rewritten into

$$\int_0^l \frac{\rho}{A(x)} dx \frac{dq}{dt} = p(0) - p(l) - F|q|q + \rho g \left[h(l) - h(0) \right] \tag{2.40}$$

where F is equal to

$$F = \frac{\rho}{2} \left(\int_0^l \frac{\partial K}{\partial x} \frac{1}{A(x)^2} dx + \int_0^l \frac{1}{4} \frac{S(x)}{A(x)^3} dx \right) \tag{2.41}$$

The two separate control volumes in the well illustrated in figure 2.1, are considered again. Equation 2.40 is integrated over a control volume of length L. If this control volume is considered to be the annulus section of the well, the term on the left side of equation 2.40 can be described as following

$$\int_0^{la} \frac{\rho}{A_a(x)} dx \frac{dq}{dt} = M_a \dot{q}_a \tag{2.42}$$

where la is the length of the annulus/well. This expression is inserted into equation 2.40 together with the topside choke pressure, the pressure at the bit, and the vertical length of the well. The flow through the annulus, will consist of the flow through the bit and the influx from the reservoir, $q_a = q_{bit} + qres$.

$$f M_a \dot{q}_a = p_{bit} - pc - F_a |(q_{bit} + q_{res})|(q_{bit} + q_{res}) - \rho_a g h_{bit} \tag{2.43}$$

Rearranging the equation obtaining an expression for the BHP:

$$p_{bit} = p_c + F_a |(q_{bit} + q_{res})|(q_{bit} + q_{res}) + M_a (\dot{q}_{bit} + \dot{q}_{res}) + \rho_a g h_{bit} \tag{2.44}$$

The same procedure can be performed on the drillpipe section of the well. The left side expression in 2.40 will then be:

$$\int_0^{ld} \frac{\rho}{A_d(x)} dx \frac{dq}{dt} = M_d \dot{q}_d \tag{2.45}$$

Equation 2.40 will together with the topside pump pressure, the pressure at the bit, and the vertical depth of the well.

$$M_d\dot{q}_d = p_p - p_{bit} - F_d|q_d|q_d + \rho_d g h_{bit} \tag{2.46}$$

Where the flow through the drill pipe, q_d, is equal to the flow through the drill bit, $q_{bit} = q_d$. Rearranging the equation to obtain the expression for BHP.

$$p_{bit} = p_p - F_d|q_{bit}|q_{bit} - M_d\dot{q}_{bit} + \rho_d g h_{bit} \tag{2.47}$$

Adding equation 2.46 and 2.43 together:

$$\begin{aligned} M_a\dot{q}_a + M_d\dot{q}_d = p_{bit} - p_c - F_a|(q_{bit}+q_{res})|(q_{bit}+q_{res}) - \rho_a g h_{bit} + p_p \\ - p_{bit} - F_d|q_{bit}|q_{bit} + \rho_d g h_{bit} \end{aligned} \tag{2.48}$$

Defining $M = M_a + M_d$

$$M\dot{q}_{bit} = p_p - p_c - F_a|(q_{bit}+q_{res})|(q_{bit}+q_{res}) - F_d|q_{bit}|q_{bit} + (\rho_d - \rho_a) g h_{bit} \tag{2.49}$$

Equation 2.44 and 2.49 are combained. q_{res} is assumed to be a slowly varying parameter. This assumption leads to $\dot{q}_{bit} = 0$.

$$p_{bit} = p_c + F_a|(q_{bit}+q_{res})|(q_{bit}+q_{res}) + M_a(\dot{q}_{bit} + \dot{q}_{res}) + \rho_a g h_{bit} \tag{2.50}$$

Insertion of $\dot{q}_{bit}$ gives

$$\begin{aligned} p_{bit} = p_c + F_a|(q_{bit}+q_{res})|(q_{bit}+q_{res}) + \frac{M_a}{M}(p_p - p_c - F_a|(q_{bit}+q_{res})|(q_{bit}+q_{res}) \\ - F_d|q_{bit}|q_{bit} + (\rho_d - \rho_a) g h_{bit}) + \rho_a g h_{bit} \end{aligned} \tag{2.51}$$

$$\begin{aligned} p_{bit} = \frac{M_d}{M}p_c + \frac{M_a}{M}p_p - \frac{M_a}{M}F_d|q_{bit}|q_{bit} \\ + \frac{M_d}{M}F_a|(q_{bit}+q_{res})|(q_{bit}+q_{res}) + \left(\frac{M_a}{M}\rho_d - \frac{M_d}{M}\rho_a\right) g h_{bit} \end{aligned} \tag{2.52}$$

2.5 Model Summary

A brief summary of the important equations derived in this chapter: These equations will be the foundation of the observer presented in chapter 3 and the NMPC control scheme presented in chapter 4.

$$\frac{V_D}{\beta}\dot{p}_p = q_{in} - q_{bit} - \dot{V}_D \tag{2.53}$$

$$\frac{V_A}{\beta}\dot{p}_c = q_{bit} + q_{res} + q_{bp} - q_{out} - \dot{V}_A \tag{2.54}$$

$$M\dot{q}_{bit} = p_p - p_c - F_a|(q_{bit}+q_{res})|(q_{bit}+q_{res}) - F_d|q_{bit}|q_{bit} + (\rho_d - \rho_a)gh_{bit} \tag{2.55}$$

$$\rho = \rho_0 + \frac{\rho_0}{\beta}(p - p_0) \tag{2.56}$$

$$\begin{aligned} p_{bit} = {} & \frac{M_d}{M}p_c + \frac{M_a}{M}p_p - \frac{M_a}{M}F_d|q_{bit}|q_{bit} \\ & + \frac{M_d}{M}F_a|(q_{bit}+q_{res})|(q_{bit}+q_{res}) + \left(\frac{M_a}{M}\rho_d - \frac{M_d}{M}\rho_a\right)gh_{bit} \end{aligned} \tag{2.57}$$

2.6 Drill bit

The drill bit will be equiped with a check valve to prevent flow from the annulus to the drillpipe; $q_{bit} \geq 0$. This check valve will e.g be active during the pipe connection procedure. If it was not present, the fluids in the well would flow up through the drillpipe during the pipe connection (The pipe connection procedure is described in section 5.4. The check valve is a physical limitation that will affect the model. When $q_{bit} = 0$ the equation for $\dot{q}_{bit}$ reduces to:

$$M\dot{q}_{bit} = max\left(0, p_p - p_c - F_a|q_{res}|q_{res} + (\rho_d(p) - \rho_a(p))gh_{bit}\right) \tag{2.58}$$

2.7 Reservoir

In this thesis the reservoir influx will be assumed to be equal to zero, $q_{res} = 0$. This is a major simplification and decreases the complexity of the problem. The influx from the reservoir would most likely effect the density in the well, and it is also likely that there would be gas present in the influx. A multi-phase flow is more complex than a singel-phase, and it might be necessary to use a two-phase model to adequately describe the process.

Chapter 3

Adaptive Estimation of BHP

The lack of a continuous BHP measurement rises the need of an estimation of the BHP. In this chapter a nonlinear observer based on the model derived in Chapter 2 will be presented. The nonlinear adaptive observer is originally developed in a master thesis [Øyvind Nistad Stamnes, 2007]. The observer uses only the topside measurements to estimate the flow through the bit, the friction factor in the annulus, and the difference in density between the drillpipe and the annulus. The measurements needed to performe the calculations are the topside pump pressure, the choke differential pressure and the pump flows. An alternative approach to estimating the BHP can be found in Nygaard et al. [2006], where the BHP is estimated by *extended*, *ensemble* and *uncented* Kalman filter.

3.1 Model

The observer is dependent upon the model derived in chapter 2 to estimate the BHP.

$$\dot{p}_p = \frac{\beta_D}{V_D}\left(q_{in} - q_{bit} - \dot{V}_D\right) \tag{3.1}$$

$$\dot{p}_c = \frac{\beta_A}{V_A}\left(q_{bit} + q_{res} + q_{bp} - q_{out} - \dot{V}_A\right) \tag{3.2}$$

$$\dot{q}_{bit} = \frac{1}{M}(p_p - p_c) - \frac{F_a - F_d}{M}|q_{bit}|q_{bit} + \frac{\rho_d - \rho_a}{M}gh_{bit} \tag{3.3}$$

In Øyvind Nistad Stamnes [2007] the author has chosen to adapt two parameters. The parameters are defined as following:

$$\theta_1 = \frac{F_a - F_d}{M} \tag{3.4}$$

$$\theta_2 = \frac{\rho_d - \rho_a}{M} \tag{3.5}$$

The purpose of the first parameter, θ_1, is to obtain an estimation of the friction in the annulus, F_a. The friction in the annulus would be affected by the roughness of the annulus-walls, and it would also be dependent on influx of reservoir fluids.

The purpose of the second parameter, θ_2, is to obtain an estimation of the difference in density between the drillpipe and the annulus section of the well. These two parameters are inserted into equation 3.3.

$$\dot{q}_{bit} = \frac{1}{M}(p_p - p_c) - \theta_1 |q_{bit}| q_{bit} + \theta_2 h_{bit} \tag{3.6}$$

The equation of the BHP has previously been defined to be:

$$p_{bit} = p_c + F_a |q_{bit}| q_{bit} + M_a \dot{q}_{bit} + \rho_a g h_{bit} \tag{3.7}$$

The new expression for $\dot{q}_{bit}$ is inserted into equation 3.7:

$$p_{bit} = p_c + (M\theta_1 - F_d)|q_{bit}|q_{bit} + M_a(\frac{1}{M}(p_p - p_c) - \theta_1 |q_{bit}|q_{bit} + \theta_2 h_{bit}) + (\rho_d g - M\theta_2)h_{bit} \tag{3.8}$$

This equation will later be used to estimate the BHP.

3.2 Stability

The observer of the BHP is derived with an approach motivated by a method described in Tan et al. [1998]. Inspired by this article; the change of coordinates is defined as:

$$\xi_1 = q_{bit} + l_1 p_p \tag{3.9}$$

where l_1 is a feedback gain. The observer equations will not be derived here, but the reader may refer to Øyvind Nistad Stamnes [2007] for a complete insight to the observer derivation and the proof of stability. When the approach in equation 3.9 is used, exponential stability can be guaranteed. The stability is proved through Lyapunov analysis.

3.3 Observer Equations

The most important results from Øyvind Nistad Stamnes [2007] is summarized in table 3.1. This equations are implemented directly to estimate the BHP in the following simulations.

Observer	$\rho_d(p) = \rho_{d,0} + \frac{\rho_{d,0}}{\beta}(p - p_0)$ $\hat{p}_{bit} = p_c + (M\hat{\theta}_1 - F_d)\lvert\hat{q}_{bit}\rvert\hat{q}_{bit} + M_a(\frac{1}{M}(p_p - p_c) - \hat{\theta}_1\lvert\hat{q}_{bit}\rvert\hat{q}_{bit} + \epsilon$ $+\hat{\theta}_2 h_{bit}) + (\rho_d(p)g - M\hat{\theta}_2)h_{bit}$ $\hat{q}_{bit} = \hat{\xi}_1 - l_1 p_p$ $\dot{\hat{\xi}}_1 = -l_1\frac{\beta_d}{V_d}\hat{q}_{bit} - \hat{\theta}_1\lvert\hat{q}_{bit}\rvert\hat{q}_{bit} + \hat{\theta}_2 h_{bit} + \frac{1}{M}(p_p - p_c) + l_1\frac{\beta_d}{V_d}Q_{in}$ $\hat{\xi}_1(0) = \hat{q}_{bit}(0) + l_1 p_p(0)$
Adaptive law	$\dot{\hat{\theta}} = \dot{\hat{\sigma}} - \eta(\hat{q}_{bit}, h_{bit})$ $\dot{\hat{\sigma}} = -l_1\frac{\partial\eta}{\partial\hat{q}_{bit}}\frac{\beta_d}{V_d}(q_{in} - \hat{q}_{bit}) + \frac{\partial\eta}{\partial\hat{q}_{bit}}\dot{\hat{\xi}}_1 + \frac{\partial\eta}{\partial h_{bit}}\dot{h}_{bit}$ $\hat{\sigma}(0) = \hat{\theta}(0) + \eta\left(\hat{q}_{bit}(0), h_{bit}(0)\right)$ $\eta(\hat{q}_{bit}, h_{bit}) = \Gamma\begin{bmatrix} \frac{\lvert\hat{q}_{bit}\rvert^3}{3l_1\frac{\beta_d}{V_d}} \\ -\frac{h_{bit}\hat{q}_{bit}}{l_1\frac{\beta_d}{V_d}} \end{bmatrix}$ $\frac{\partial\eta}{\partial\hat{q}_{bit}} = \Gamma\begin{bmatrix} \frac{\lvert\hat{q}_{bit}\rvert\hat{q}_{bit}}{l_1\frac{\beta_d}{V_d}} \\ -\frac{h_{bit}}{l_1\frac{\beta_d}{V_d}} \end{bmatrix}$ $\frac{\partial\eta}{\partial h_{bit}} = \begin{bmatrix} 0 \\ -\frac{\hat{q}_{bit}}{l_1\frac{\beta_d}{V_d}} \end{bmatrix}$
Design variables	Observer gain $l_1 > 0$ Adaption gain: $\Gamma = \Gamma^T > 0$ Initial conditions: $\hat{q}_{bit}(0)$ and $\hat{\theta}(0)$

Table 3.1: Summary of Adaptive Observer

3.4 Weaknesses

There are some weaknesses with the presented observer. As stated in Øyvind Nistad Stamnes [2007] there is an unsolved issue in connection with the case of zero flow, $q_{bit} = 0$. Stability can no longer be proven, and the author presents an ad-hoc solution to overcome the problem. The solution presented is a small modification to the observer; when the following conditions occurs:

$$q_{bit} = 0 \text{ and } (\frac{1}{M}(p_p - p_c) + \theta_2 h_{bit}) < 0 \tag{3.10}$$

these modifications are made to the observer:

$$\dot{\hat{\xi}}_1 = l_1 \frac{\beta_d}{V_d} q_{in} \tag{3.11}$$

$$\hat{p}_{bit} = p_c + (\rho_d(p)g - M\hat{\theta}_2)h_{bit} \tag{3.12}$$

An other important issue is that the observer is sensitive to errors in the assumption of the drillpipe friction parameter, F_d. The observer is designed to estimate the friction in the annulus and not the drillpipe. This choice of design can be justified through the assumption that the friction in the annulus would be more unpredictable and will have larger variations than the friction in the drillpipe.

One of the disadvantages with this observer design, is that the measurement of the BHP is ignored. When there is a sufficent flow in the well, the measurement of the BHP is sendt to the surface by an MPT system. The MPT system has a low bitrate, and the measurement will be disturbed by noise. Even so, the observer should be redesigned to take this measurement into consideration. The time elapsed between every sample of the BHP will in this report be assumed to be constant, and the time elapsed between each sample will be denoted T_m. In the following, a minor modification to the observer will be presented. The main objective of this modification is to cancel the difference between the estimated and the measured BHP.

$$\delta = K_\epsilon(y - \hat{y}) = K_\epsilon(p_{bit} - \hat{p}_{bit}) \tag{3.13}$$

Due to sensitivity to noise, the size of K_ϵ should be small (approximately: $K_\epsilon < 0.1$). If ϵ where to be added directly to equation 3.15 it would result in a discontinuity in the observer each time a new measurement is obtained. To avoid this, the time elapsed between two samples is used to smooth out the estimate. At each time interval a fraction is added to the observer.

$$\epsilon_{k+1} = \epsilon_k + \frac{\delta}{T_m} \tag{3.14}$$

Adding ϵ_k to equation 3.15 will reduce the difference between the estimated and measured BHP.

$$p_{bit} = p_c + (M\theta_1 - F_d)|q_{bit}|q_{bit} + M_a(\frac{1}{M}(p_p - p_c) - \theta_1|q_{bit}|q_{bit} + \theta_2 h_{bit}) + (\rho_d g - M\theta_2)h_{bit} + \epsilon \quad (3.15)$$

However, adding this term to the equation, will give the same effect as alternating the density in the well. It has not been the author's purpose to develop a more advanced observer, but as a suggestion for future development of the observer, the BHP could either be used to estimate the density in the well, ρ, or the fricton in the drillpipe, F_d.

Another issue is that the relationship between the density of the mud and the pressure in the well is ignored. As discussed in the modeling chapter, the variations in density due to pressure, can be approximated by:

$$\rho(p) = \rho_0 + \frac{\rho_0}{\beta}(p - p_0) \quad (3.16)$$

In the implementation the pressure at time k is used to calculate the density at time k+1, which again is used to calculate the pressure at time k+1.

The observer also has a problem with observability when estimating two parameters. The θ_1 and θ_2 solution found would converge to a final value, but the value found is most likely not the correct value. Because of the problem with observability, the adaption of θ_2 will be turned off, and the value kept constant through the simulations.

3.5 Verifying the Observer

The observer's ability to estimate the pressure correctly is essential for controlling purposes. The observer was analyzed in Øyvind Nistad Stamnes [2007], but since the observer has been modified, some simulations will be run to analyze the performance of the modified observer. The scenario that will be used to test the observer, is the pipe connection procedure. The procedure can be found in section 5.4. The following simulations will be run without the presence of a controller (*open-loop*).

In the first simulation, presented in figure 3.1 , K_ϵ is set equal to zero, and the density is held constant, independent of the pressure variations. When K_ϵ is set equal to zero, the BHP measurement is ignored. The observer is equal to the original observer with this parameter set. The resulting parameters can be found in table 5.1.

The result of this simulation can be found in figure 3.1. It can be observed from the simulations that the observer presents a good estimation of the BHP during a pipe connection. However, it is a small deviation between the estimated pressure, with the set of parameters used, and the BHP measured. The measured BHP is presented by a commercial simulator. (See section 5.1 for more information on the simulator used).

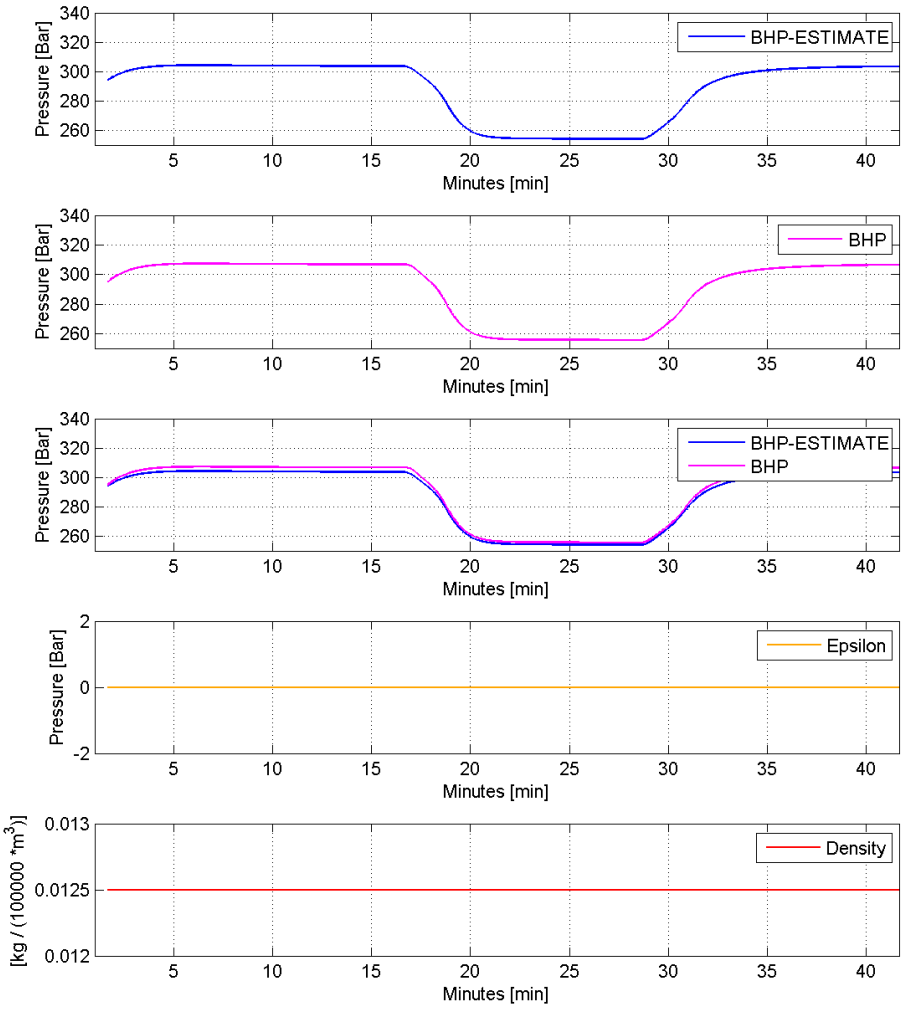

Figure 3.1: Open-loop pipe connection: Original Observer

K_ϵ is kept equal to zero in the second simulation. But in this simulation the density is set to be pressure dependent. Equation 3.16 is included in the observer. The result of this simulation can be found in figure 3.2. It can be observed that implementing a pressure dependent density represents a minor improvement to the estimation of the BHP. The variations in density are small, but when the hydrostatic pressure is calculated, the density is multiplied with gravity and the vertical height of the well. Multiplying with gravity and height will in this specific well represent a factor of 20 000. If the density is increased from 0.0125 to 0.0126, the hydrostatic pressure will be increased by 2.0 bars.

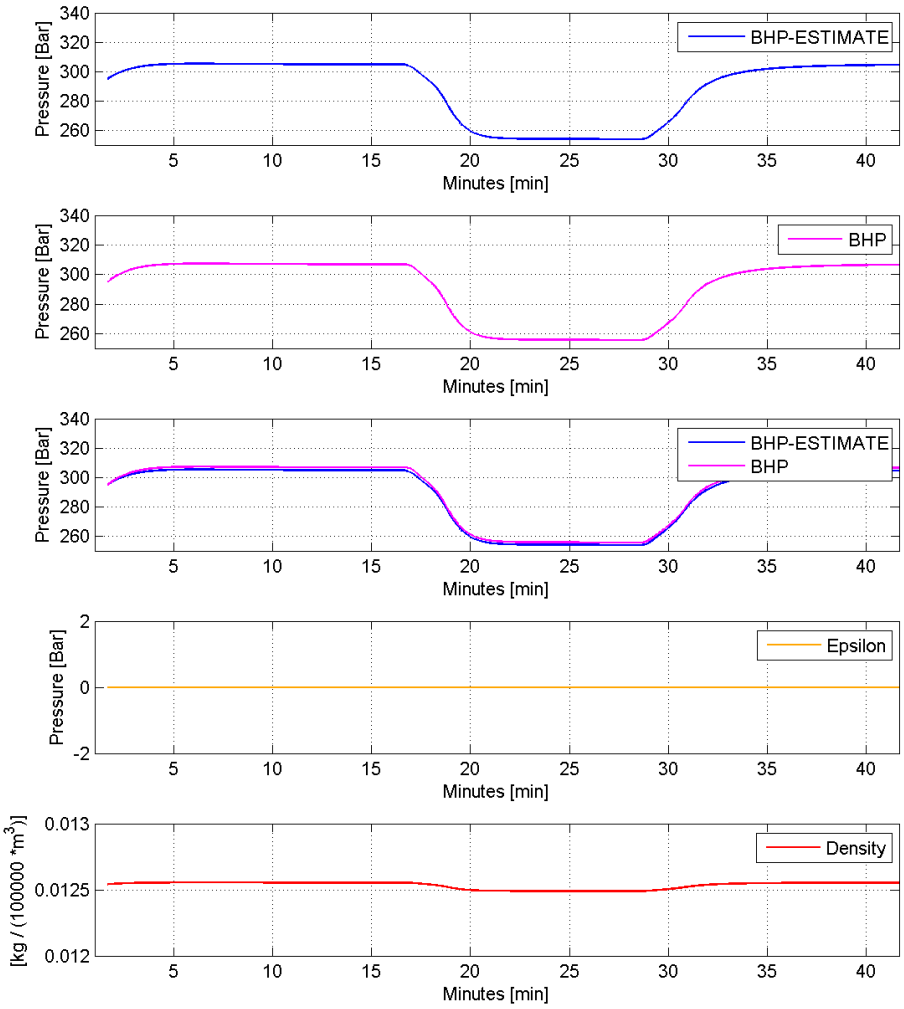

Figure 3.2: Open-loop pipe connection: Density is pressure dependent

K_ϵ is set equal to 0.05 in the third simulation, and the density is still pressure dependent. The result of the simulation is presented in figure 3.3. The BHP measurement is assumed to reach the surface once every 30 sec when the flow is above 500 [l/min], and noise will be absent in the measurement in this simulation. When the BHP measurement is used, the performance of the observer is further improved.

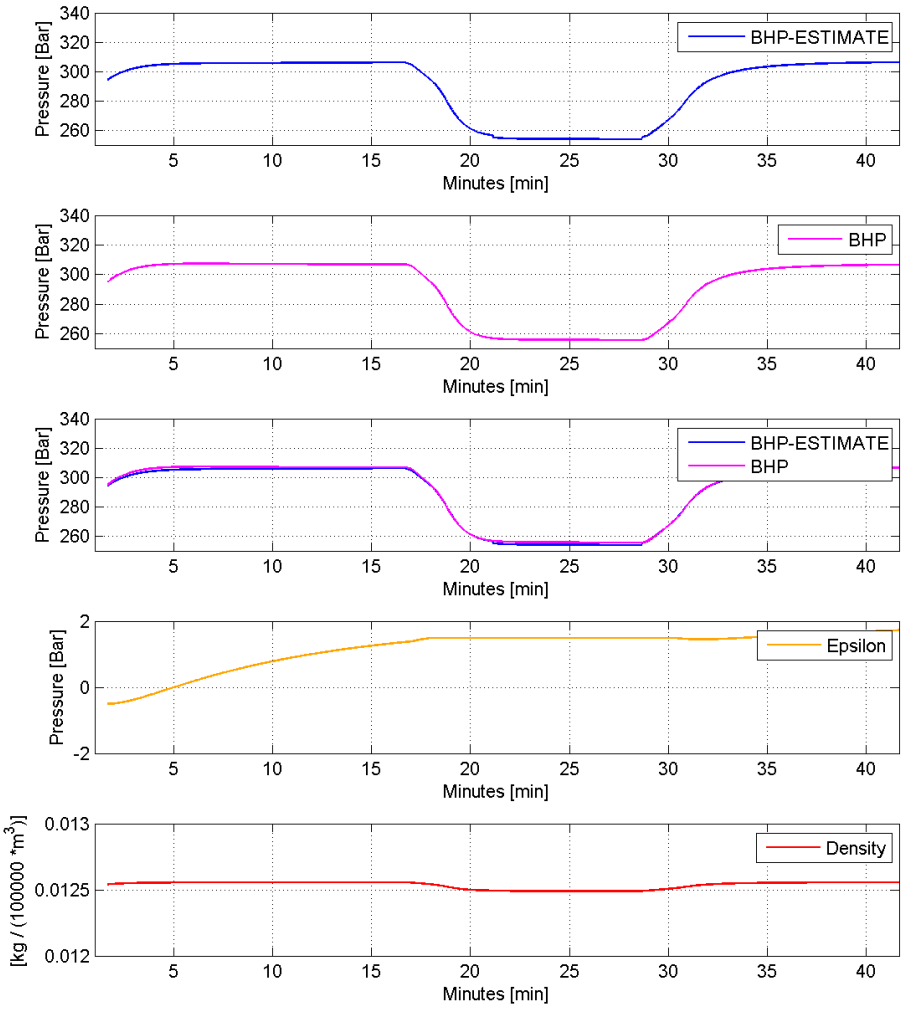

Figure 3.3: Open-loop pipe connection: Density is pressure dependent. BHP measurement is used.

In the fourth and final simulation the observer will be the same as in the above simulation. In this simulation noise will be present, and will make the BHP measurement less reliable. The noise will be generated by a pseudo-random MatLab function, *randn()*. Pseudo-random values will be drawn from a normal distribution with mean zero and standard deviation of one. The results are presented in figure 3.4. The performance of the observer is not significantly reduced with this set of parameters, even though the BHP measurement is influenced by noise. Increasing K_ϵ will increase the observer's sensibility to noise. If there are noise present, as assumed in this simulation, K_ϵ should be chosen with care.

The simulations illustrate that the modifications made to the observer result in a slightly increased performance. These modifications will be present in all following simulations. The noise generator will be turned off in all simulations in chapter 5.

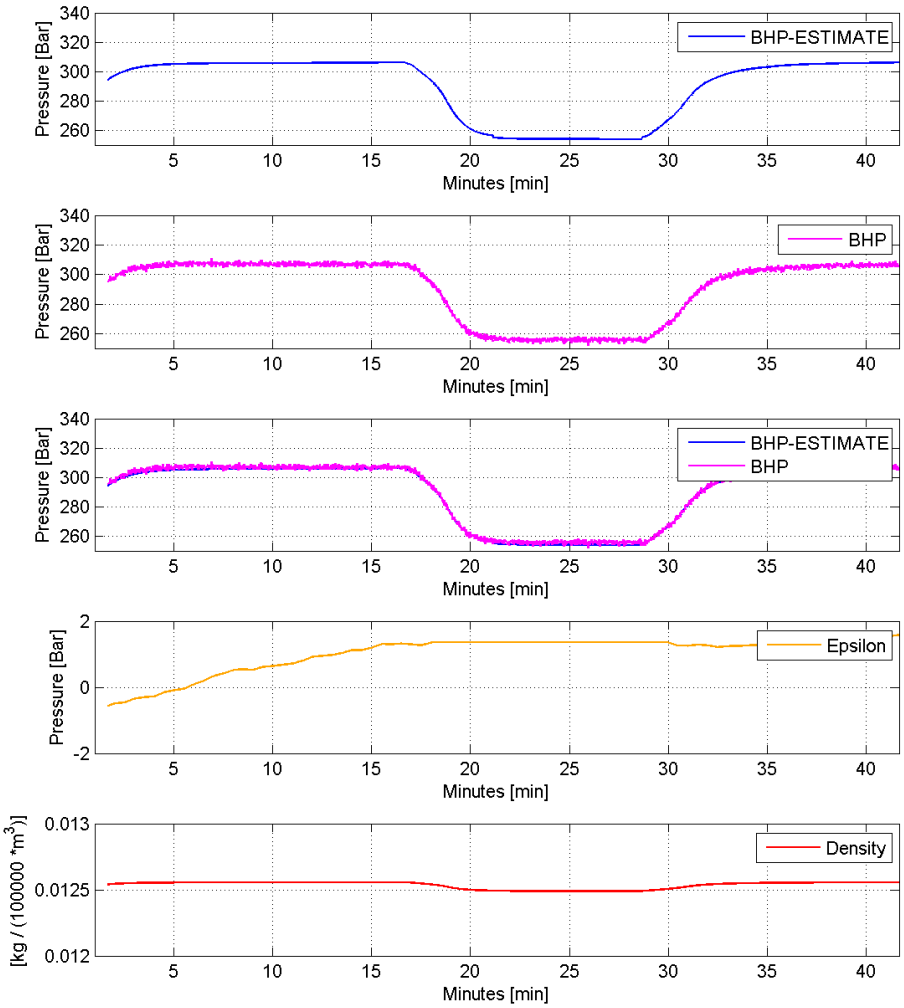

Figure 3.4: Open-loop pipe connection: Sensitivity to noise

Chapter 4

Model Predictive Control

MPC is the only advanced controller which has made a significant impact on the industrial control engineering. In section 4.1 the history of the MPC controller will be presented. The MPC controller stands out from other advanced controllers by its history within the industrial community. The controller did not have its origin within theoretical communities, which is the case of most advanced controllers. Predictive control was developed and used in the industry as an effective tool for dealing with multivariable constrained control problems. Mayne et al. [2000] defines MPC as following:

> *'Model predicitve control (MPC) or receding horizon control(RHC) is a form of control in which the current control action is obtained by solving on-line, at each sampling instant, a finite horizon open-loop optimal control problem, using the current state of the plant as the initial state; the optimization yields an optimal control sequence and the first control in this sequence is applied to the plant.'*

The purpose of choosing an MPC control scheme to control any process, is to optimize the outcome. An MPC controller enables the system to operate closer to the process boundaries, and an increase in profit would be the main objective of such an implementation. The MPC controller can be used to optimize the process directly on setpoints (optimizing PI-controllers), and on a high-level optimization of the full process. Qin and Badgwell [2003] lists the main objective of an MPC controller in prioritized order as following:

1. Prevent violation of input and output constraints

2. Drive the CVs to their steady-state optimal values

3. Drive the MVs to their steady-state optimal values using remaining degrees of freedom

4. Prevent excessive movement of MVs

5. When signals and actuators fail, control as much of the process as possible

4.1 Historical Development of MPC

A short survey of industrial model predictive control technology is presented in this section. The reader may refer to Qin and Badgwell [2003] for a more thorough presentation on the topic. The historical presentation presented here is a brief summary of the work of Qin and Badgwell [2003].

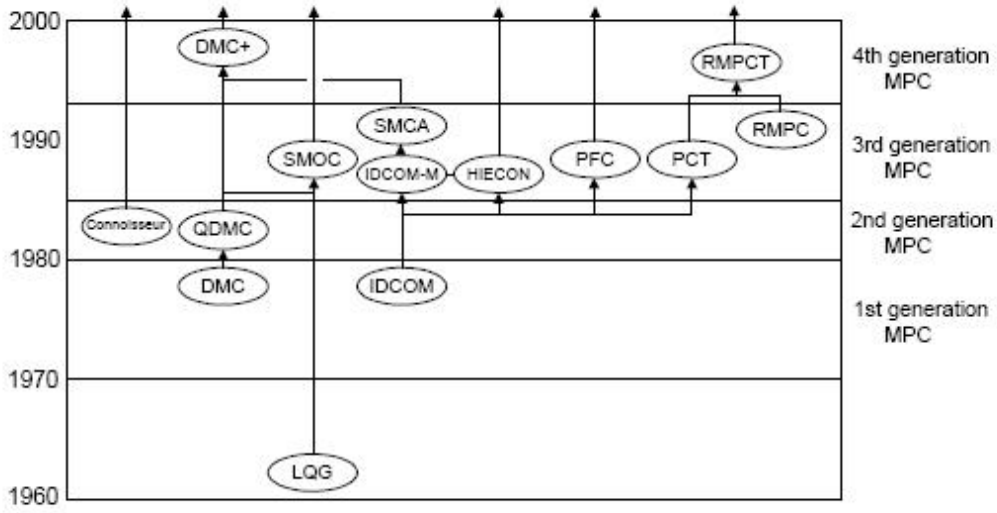

Figure 4.1: Timeline: MPC technologies Qin and Badgwell [2003]

4.1.1 LQG

The development of modern control concepts can be traced back to the work of Kalman in the early 60's, and the reader may refer to relevant articles as Kalman [1960a] and Kalman [1960b] for a in-depth description of the linear quadratic gaussian (LQG) controller. The LQG represents an automated method to compute a state-feed back controller, $u = k_c x$. At every timestep

the output measurement is used to calculate an optimal state estimate. Then the optimal input is calculated, and the kalman filter gain K_c is found be solving a dual Ricatti equation.

The LQG controller did not have a significant impact on control technology development in the process industry. The main reasons for this are listed here, and a more thorough discussion on that topic can be found in Richalet et al. [1976].

- constraints
- process nonlinearities
- model uncertainty (robustness)
- unique performance criteria
- cultural reasons (people, education, etc)

4.1.2 IDCOM

The first MPC application is refered to as IDCOM, an acronym for *Identification and Control*, and can be found presented in Richalet et al. [1976], and summarized in Richalet et al. [1978]. The authors described their approach as *model predicitve heuristic control* (MPHC). In Qin and Badgwell [2003] the following list of distinguishing features of the IDCOM approach are presented:

- impulse response model for the plant
- quadratic performance objective over a finite predicition horizon
- future plant output behavior specified by a reference trajectory
- input and output constraints included in the formulation
- optimal inputs computed using a heuristic iterative algorithm, interpreted as the dual of identification

In Richalet et al. an input-output represention are chosen, and the inputs are refered to as manipulative variables (MVs) and disturbance variables (DVs), and the outputs are refered to as controlled variables (CVs). The MVs are adjusted by the controller, and the DVs are assumed to be unavailable for control. The relationship between the process inputs and outputs are

described by a discrete-time finite impulse respons (FIR) model. If the singel input singel output (SISO) scenario is considered, the FIR model looks like:

$$y_{k+j} = \sum_{i=1}^{N} h_i u_{k+j-i} \tag{4.1}$$

where h_i are the impulse response coefficients. This approach uses the linear combination of past inputs to calculate a predicted output. As stated in Qin and Badgwell [2003], this approach is only possible for stable plants.

In Richalet et al. another important point on dynamic optimization was made. They stated that dynamic control must be embedded in a hierarchy of plant control functions to be efficient. Four levels of control are described:

- Level 3: Time and space scheduling of production
- Level 2: Optimization of setpoints to minimize costs and ensure quality and quantity of production
- Level 1: Dynamic multivariable control of the plant
- Level 0: Control of ancillary systems; PID control of valves

The conclusion made in Richalet et al., is that the real economic benefits come at level 2, where better dynamic control allows the operational point to be moved closer to the constraints, whitout violating them.

4.1.3 DMC

Dynamic Matrix Control (DMC) was developed by Shell engineers in the early 70's, and can found published in Cutler and Ramaker [1979]. Some of the key features of the DMC approach are:

- Linear step response model for the plant
- Quadratic performance objective over a finite prediction horizon
- Future plant output behavior specified by trying to follow the setpoint as closely as possible
- Optimal inputs computed as the solution to a least-squares problem

If the SISO case is considered again, the step response model takes the following form:

$$y_{k+j} = \sum_{i=1}^{N-1} s_i \Delta u_{k+j-i} + s_N u_{k+j-N} \tag{4.2}$$

where s_i are the step response coefficients. DMC uses the principle of superposition; the predicive future outputs are described as a linear combination of the future input moves.

The *IDCOM* and the *DMC* applications are considered to be first generation MPC applications. They made a significant impact on industrial process control.

4.1.4 QDMC

The *IDCOM* and the *DMC* applications had a weakness in constraints handling. However, they offered excellent control for unconstrainted multivariable processes. Engineers at SHELL suggested formulating the DMC algorithm as a quadratic programming (QP) problem. This approach was first presented in Cutler et al. [1983]. This method is called quadratic dynamic matrix control (QDMC). Key features of this approach are:

- Linear step response model of the plant
- Quadratic performance objective over a finite prediction horizon
- Optimal inputs computed as the solution to a quadratic program

QDMC is considered to be a second generation MPC application. QDMC formulated the problem as a standard QP, which could easily be solved by commercial available software. QDMC provided a systematic way of handling input and output constraints.

After the sucsess of the second generation MPC applications, the technology gained wider acceptance, and problems handled by MPC technology grew larger and more complex. However, issues like the abscence of a clear procedure on how to handle an infeasible solution, motivated control engineers to further develop the technology, and new third generation solutions like *Shell Multivariable Optimizing Controller* (SMOC)[Yousfi and Tournier, 1991] emerged. This generation of MPC controllers distinguishes between different level of constraints: soft, hard and ranked. They provide a way to recover from an infeasible solution, and allows for a wider range of process dynamics: stable, integrating and unstable.

Todays commercial available MPC solutions are often referred to as fourth generation MPC. This include, among others, *DMC-plus* and *RMPTCT*. The latter is Honeywell's MPC solution. These fourth generation MPC applications provide a Windows-based graphical interface, they have multiple optimization levels to address prioritized control objectives, direct consideration of model uncertainty, and additional flexibility in the steady-state target optimization.

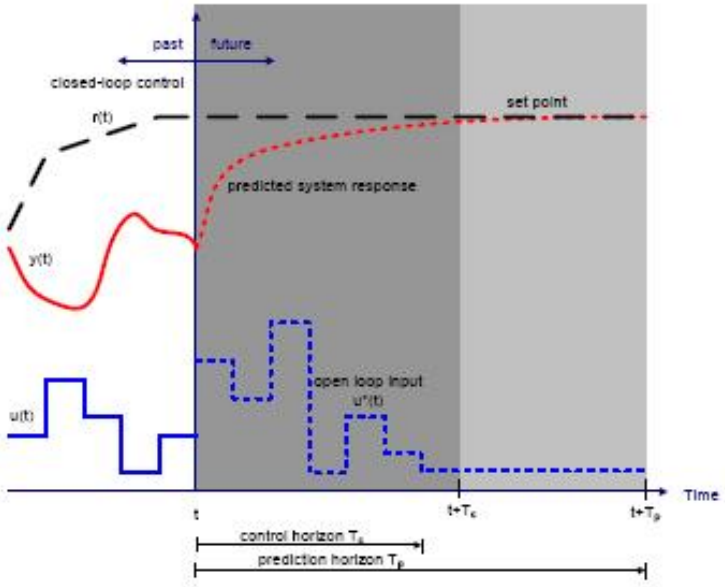

Figure 4.2: Example of MPC Torpe [2007]

4.2 Nonlinear Model Predictive Control

Most running MPC applications are based on linear experimental models. In many cases the linear models make up an adequate representation of the process, and are well suited for control purposes. However, since the 90's there has been a steady increase in interest from the control theoreticians as well as control practitioners in nonlinear model predicitve control (NMPC). The demand and wish to push the boundaries of the controller to increase profit and process performance has been the motivation to an increased interest in nonlinear control. As Rawlings [2000] states:

> *'The fundamentals in any process control problem-conservation of mass, momentum, and energy; considerations of phase equilibria; relationships of chemical kinetics and properties of final products- all introduce nonlinearity into the process description.'*

In this section some important aspects of NMPC will be discussed. The discussion is based on the work of Allgöwer et al. [2004], and the notation used here will follow his example. Allgöwer et al. [2004] present a list of key characteristics and properties of NMPC:

- NMPC allows the direct use of nonlinear models for prediciton.
- NMPC allows the explicit consideration of state and input constraints.

- In NMPC a specific time domain performance criteria is minimized on-line.
- in NMPC the predicted behavior is in general different from the closed loop behavior.
- For the application of NMPC typically a real-time solution of an open-loop optimal control problem is necessary
- To perform the prediciton, the system states must be measured or estimated.

NMPC schemes based on continuous differential equations will be considered in this report. Information on discrete NMPC schemes can be found in Mayne et al. [2000] and Rawlings [2000]. Systems in the following form will be considered.

$$\dot{x}(t) = f(x(t), u(t)),\ x(0) = x_0 \tag{4.3}$$

subject to input and state constraints of the form:

$$u(t) \in U,\ \forall t \geq 0, \tag{4.4}$$

$$x(t) \in X,\ \forall t \geq 0. \tag{4.5}$$

$x(t) \in \mathbf{R}^n$ and $u(t) \in \mathbf{R}^m$ denotes the state and input vector. In a NMPC application, the following finite horizion open-loop optimal control problem is solved at every sampling instant:

$$\min {}_{\bar{u(\cdot)}} J(x(t), \bar{u}(\cdot)) \tag{4.6}$$

subject to:

$$\dot{\bar{x}}(\tau) = f(\bar{x}(\tau), \bar{u}(\tau)),\ \bar{x}(t) = x(t) \tag{4.7a}$$
$$\bar{u}(\tau) \in U,\ \forall \tau \in [t, t + T_c] \tag{4.7b}$$
$$\bar{u}(\tau) = \bar{u}(t + T_c),\ \forall \tau \in [t + T_c, t + T_p] \tag{4.7c}$$
$$\bar{x}(\tau) \in X,\ \forall \tau \in [t, t + T_p] \tag{4.7d}$$

with the cost function:

$$J(x(t), \bar{u}(\cdot)) := \int_t^{t+T_p} F(\bar{x}(\tau), \bar{u}(\tau)) d\tau \tag{4.8}$$

T_p and T_c denotes the prediciton and control horizion.

$$F(x,u) = (x - x_s)^T Q(x - x_s) + (u - u_s)^T R(u - u_s) \tag{4.9}$$

In equation 4.9, x_s and u_s denote the desired reference trajectories. The latter can be both time-varying or constant. The matrices Q and R are positive definite matrices, and weighten the deviation from the optimal trajectories.

4.2.1 Calculation Issues

NMPC requires a repeated online-calculation of a nonlinear programming(NP) problem. A linear MPC application requires only an on-line solution to a QP problem. Solving a QP problem is easily done with commercial software, and the possibility of efficient on-line calculation is one of the main reasons for the sucsess of linear MPC applications. Solving a NP is not straightforward, and requires much computational power. According to Allgöwer et al. [2004] the computational expensivness of NP solving was and still is one of the key limitations on a successful practical implementation of NMPC.

4.2.2 Stability and Robustness

The research on MPC stability has become a relativily mature field, and the important factors of stability have been isolated and employed. The definition of stability and robustness will follow the example of Skogestad and Postlethwaite [2005], where stability is defined to be the case of nominal stability. The plant is assumed to be modelled perfectly. Robustness is defined to be robust stability, meaning stability of all the plants within the uncertainty set.

The most intuitive method to ensure stability is to use a infinte horizon controller. At a random sampling instant, the open-loop input and state trajectories calculated by the NMPC scheme, are in fact equal to the closed-loop response of the system. If the first sequence is applied to the system, the remaining parts of the trajectory is still the optimal solution. This implies convergence of the closed-loop. A more detailed description of the infinte horizon NMPC can be found in Mayne et al. [2000].

If the horizion is finite, there exist different solutions to ensure stability. These approaches mainly alternate the original NMPC scheme by including additional equality or ineequality constraints. These additonal constraints, and corresponding penalties, are not related to the physical process. They are implemented with the singel purpose of guaranteeing stability. One method to enforce stability is to implement a terminal equality at the end of the optimization horizon.

$$\bar{x}(t+T_p) = 0 \tag{4.10}$$

More information on this approach can be found in Mayne and Michalska [1990] and Chen and Shaw [1982]. The main drawback to this approach is that all the states have to be brought to zero within the prediction horizion. Bringing all states to zero strongly reduces the solution space of the problem. From a computational view it is almost impossible to bring all states to the exact value of zero, within a finite number of iterations. There is a strong possibilty that this method will result in an infeasible solution. (Feasibility will be discussed in section 4.2.3.) Another method to ensure stability exist, and it is a natural development of the terminal value method. Instead of defining a terminal value, a set of terminal values are defined.

$$\bar{x}(t+T_p) \in \Omega \tag{4.11}$$

Another approach is to add a terminal penalty term $E(\bar{x}(t+T_p))$ to the problem. The terminal region, Ω, and the terminal cost are often calculated off-line, such that the cost function

$$J(x(t), \bar{u}(\cdot)) = \int_t^{t+T_p} F(\bar{x}(\tau), \bar{u}(\tau))d\tau + E(\bar{x}(t+T_p)) \tag{4.12}$$

gives an upper bound on the infinite horizon cost. This gurantees a decrease in the value function. For this to be taken into consideration in the optimization, the problem has to be reformulated. The new problem would be:

$$\min {}_{\bar{u(\cdot)}} J(x(t), \bar{u}(\cdot)) \tag{4.13}$$

subject to:

$$\dot{\bar{x}}(\tau) = f(\bar{x}(\tau), \bar{u}(\tau)),\ \bar{x}(t) = x(t) \tag{4.14a}$$
$$\bar{u}(\tau) \in U,\ \forall \tau \in [t, t+T_p] \tag{4.14b}$$
$$\bar{x}(\tau) \in X,\ \forall \tau \in [t, t+T_p] \tag{4.14c}$$
$$\bar{x}(t+T_p) \in \Omega \tag{4.14d}$$

If the terminal penalty term E and the terminal region Ω is chosen with care, it is possible to gurantee closed-loop stability. The following theorem is found in Allgöwer et al. [2004].

Theorem 1 *Assume that:*

1. *$U \subset \boldsymbol{R}^m$ is compact. $X \subseteq \boldsymbol{R}^n$ is connected and the origin is contained in the interior of $U \times X$.*

2. *The vector field $f : \boldsymbol{R}^n \times \boldsymbol{R}^m \rightarrow \boldsymbol{R}^n$ is continuous in u and locally Lipschitz in x and satisfies $f(0,0) = 0$.*

3. *$F : \boldsymbol{R}^n \times U \rightarrow \boldsymbol{R}$ is continuous in all arguments with $F(0,0) = 0$ and $F(x,u) > 0 \forall (x,u) \in \boldsymbol{R}^n \times U \backslash \{0,0\}$.*

4. *The terminal penalty $E : \Omega \rightarrow \boldsymbol{R}$ is continuous with $E(0) = 0$ and that the terminal region Ω is given by $\Omega := \{x \in X | E(x) \leq e_1\}$ for some $e_1 > 0$ such that $\Omega \subset X$.*

5. *There exists a continuous local control law $u = k(x)$ such that $k(x) \in U$ for all $x \in \Omega$ and*

$$\frac{\partial E}{\partial x} f(x, k(x)) + F(x, k(x)) \leq 0, \ \forall x \in \Omega$$

6. *The NMPC open-loop optimal control problem 2 has a feasible solution for $t = 0$. Then for any sampling time $0 < \delta \leq T_p$ the nominal closed-loop system given by equations 4.13 and 4.14 is asymptotically stable and the region of attraction $\boldsymbol{R}$ is given by the set of states for which the open-loop optimal control problem has a feasible solution.*

The NMPC solution presented so far, is based on the assumption of a perfect match between the model and the actual system. It is not likely that there exists a perfect match, or that all disturbances are modelled perfectly. As discussed in Allgöwer et al. [2004] one can distinguish between the inherent robustness properties of NMPC and NMPC designes that takes model uncertainty into consideration. The inherent robustness is due to the similarity between NMPC and optimal control. Many studies has been carried out within this field, and results on inherent robustness can be found in Magni and Sepulchre [1997], or discrete time results in Scokaert et al. [1997].

Different NMPC schemes that take uncertainty into account are discussed in Jalali and Nadimi [2006], where the authors divide uncertainty into two main parts; model uncertainty and disturbance uncertainty. Different methods approaching the uncertainty problem, such as Linear Matrix inequality (LMI) based robust methods, Min-Max robust MPC methodes, and methods based on standard convex optimization problems are discussed.

4.2.3 Feasibility

There are usually two different types of constraints, input and output constraints. Input constraints are usually imposed by physical limitations on actuators, and these constraints will always be present. The input constraints can not be exceeded under any circumstances, and it is a advantage to include these limitations in the control law. In the well, the input constraint will be the maximum and minium valve opening.(Equivalent to a closed valve). Since the input constraints can not be exceeded, they are implemented as hard constraints.

It is sometimes desired to keep the output constraints within a operation range, due to e.g. safety, process equipment limitations or product specifications.(As discussed in Chapter 1, the BHP has a operational range within the fracture pressure and the formation pressure.)In the presence of disturbances, it can sometimes be impossible to keep the output within the constraints. If the output constraints are implemented as hard constraints, it can lead to an infeasible solution, meaning that there exists no solution to the problem. Clearly an infeasible solution and a subsequent calculation failure must be avoided in an online controller.

One solution to avoid the problem of infeasibility is described in Zheng and Morari [1995], where a slack variable is introduced. The slack variable softens the hard constraints. A corresponding quadratic penalty on exceeding the constraints are introduced, allowing the value to exceed the constraints. Increasing the penalty value will decrease the violation.

Note that it is not necessary to find an optimal solution to the optimization problem to gurantee stability. It is only necessary to find a feasible solution that reduces the value function. [Michalska and Mayne, 1993]

4.3 SEPTIC

StatoilHydro's Estimation and Prediction Tool for Identification and Control (SEPTIC) is StatoilHydros application for MPC solutions. At present there are approximatly 75 online SEPTIC applications on offshore and onshore installations in Norway and Denmark. As stated in Strand and Sagli [2003], all running SEPTIC applications have been implemented with experimental SISO step respons models. However, a solver for NMPC has been developed and implemented in to SEPTIC. The algorithm can be found described in Meum [2007] and Torpe [2007], and a brief summary of the method will be given here. Their approach is based on a control algorithme presented in de Oliveira and Biegler [1995], where the following rutine is used:

1. The iteration count for the QP subproblem is set to zero
2. Starting with the initial conditions, calculate the input sensitivity for the nominal trajectory
3. Solve the QP sub problem, and find the search direction
4. Run a linesearch algorithme to find the appropriate step length
5. Control wether or not the convergence criteria have been satisified. If satisfied, the first element in the input trajectory is applied to the system.
6. If the convergence criteria are still not satisfied, check the QP iteration count. If it is below the maximum allowed iterations, go back to step 2. If the maximum iterations are reached, the algorithme is brought to a halt, and the best input trajectory is returned.

4.3.1 Sensitivity

The next step is to calculate the sensitivity. In Septic, the sensitivities from input to output are calculated directly by simulating the system from t_k to t_{k+Tp}. The inputs are pertubated with a small, finite value. The changes in the outputs are obtained, and the sensitivity are calculated. The perturbation value must be chosen with care. A too small pertubation may be sensitive to noise, and a too large perturbation may result in inaccurate sensitivity function, which can cause less accurate control or stability problems. A deeper discussion on the topic of calculating sensitivity can be found in Silva and Oliveira [2002].

4.3.2 QP Solver

Schittkowski [2005] describes a Fortran subroutine QL, which solves strictly convex QP problems. The problem is solved subject to linear equality and inequality constraints by the primal-dual method described in Goldfarb and Idnani [1983]. The main advantage of the primal-dual method is that there is no need for a comprehensive search of a feasible starting point. The code solves the following strictly convex QP problem

$$\min \quad \tfrac{1}{2}x^T Q x + d^T x \tag{4.15a}$$

$$a_j^T x + b_j = 0 \ , \ j = 1, ..., m_e \tag{4.15b}$$

$$a_j^T x + b_j \geq 0 \ , \ j = m_e, ..., m \tag{4.15c}$$

where Q is a positive definite matrix. When solving the problem, violated constraints are added to an active set until the optimal solution is found. At each step, the minimal object function subject to the new active set is found. If all linear constraints and bounds are fullfilled, the optimal solutions are found, and the calculations terminate.

The fortrant code presented in Schittkowski [2005] has earlier been rewritten into C++, and implemented as the QP solver in SEPTIC.

4.3.3 Linesearch

When the original NP problem is approximated with QP sub problems, there is a posibility of the approximation beeing unsatisfactory, and that the solution found may cause the algorithme to diverge, whereupon a linesearch algorithme is needed. Nocedal and Wright [1999] present a backtracking linesearch algorithme, where a full step is first considered. Then smaller steps are considered until an acceptible step length is found.

`Choose` $\hat{\alpha} > 0$, ϵ,c $\in (0,1)$; `set` $\alpha \leftarrow \hat{\alpha}$;
`Repeat until` $f(x_k + \alpha p_k) \leq f(x_k) + c\alpha \nabla f_k^T p_k$
$\alpha \leftarrow \epsilon\alpha$
`end(repeat)`
`Terminate with` $\alpha_k = \alpha$

where p_k is the search direction. This backtracking linesearch algorithme is implemented in SEPTIC with only minor modifications.

4.3.4 Convergence

In this step of the algorithme it must be decided whether or not the convergence criteria is fullfilled. Different convergence criterias can be considered, such as linearization error, change in object function and change in input parameters. The convergence criterium which is implemented in SEPTIC is changes of the input parameters. The explicit criterium used is:

$$\sum_k ||\Delta u_k||^2 < MV_{norm} \tag{4.16}$$

where MV_{norm} is the convergence criterium. The norm should be given a small enough value to ensure that a sufficient number of QP's are solved at each iteration.

4.4 Implementation

To predicit the future behavior of the well system, the equations developed in chapter 2 and the observer equations presented in chapter 3 are used. The equations are restated here. At each timestep the future pump and choke pressure are calculated using the differential equations 4.17 and 4.18, where the volume of the drillpipe and the annulus is assumed to be constant.

$$\frac{V_D}{\beta}\dot{\hat{p}}_p = q_{in} - \hat{q}_{bit} \tag{4.17}$$

$$\frac{V_A}{\beta}\dot{\hat{p}}_c = \hat{q}_{bit} + q_{bp} - C_d u\sqrt{\frac{2\hat{p}_c}{\rho(p)}} \tag{4.18}$$

where $u = A(x)$. Equation 4.18 is a combination of equation 2.29 and 2.13. The linear simplified density function is used to predict the future density

$$\hat{\rho}_d = \rho_{d,0} + \frac{\rho_{d,0}}{\beta_d}(\hat{p}_{bit} - p_0) \tag{4.19}$$

The future value of $\hat{q}_{bit}$ is not known, and has to be calulated. To calculate the value, the observer equations are used to predict the future behavior. And with the help of equation 4.20 - 4.22, $\hat{q}_{bit}$ is predicited.

At each timestep the future behaviour of the system is predicted through the prediction horizon. During this prediciton horizon the value of the parameter θ_1 is held constant. The prediction will start with initial conditions equal to the current state of the process.

$$p_{bit} = p_c + (M\theta_1 - F_d)|q_{bit}|q_{bit} + M_a(\frac{1}{M}(p_p - p_c) - \theta_1|q_{bit}|q_{bit} + \theta_2 h_{bit}) + \rho_d(p)gh_{bit} \tag{4.20}$$

$$\hat{q}_{bit} = \hat{\xi}_1 - l_1 p_p \tag{4.21}$$

$$\dot{\hat{\xi}}_1 = -l_1\frac{\beta_d}{V_d}\hat{q}_{bit} - \hat{\theta}_1|\hat{q}_{bit}|\hat{q}_{bit} + \hat{\theta}_2 h_{bit} + \frac{1}{M}(p_p - p_c) + l_1\frac{\beta_d}{V_d}Q_{in} \tag{4.22}$$

As discussed in section 3.4, these equations are not valid at zero flow. Again the same method handling the issue is used. When

$$q_{bit} = 0 \text{ and } (\frac{1}{M}(p_p - p_c) + \theta_2 h_{bit}) < 0 \tag{4.23}$$

the following modifications are made to the prediction:

$$\dot{\hat{\xi}}_1 = l_1 \frac{\beta_d}{V_d} q_{in} \tag{4.24}$$

$$\hat{p}_{bit} = p_c + (\rho_d(p)g - M\hat{\theta}_2)h_{bit} \tag{4.25}$$

When implementing these models as the base of the NMPC scheme, a choice must be made which system inputs will be used to control the BHP. The available input with the fastest repsonse is the topside choke valve. The flow from both pumps can also be controlled under normal conditions. The slowest variable to control the BHP is the density of the mud. When changing the composition of the mud, the entire drillpipe and annulus has to be filled up with new mud, before the new steady-state is obtained. Since there are more available inputs then variables to control (sometimes refered to as a fat plant), an optimal value of the CVs could be set. However, since the main objective in this report is to focus on the pipe connection procedure (described in section 5.4), where the main pump has to be shut down, the pumps are modelled as disturbances. And since changing the composition of the density is a very slow way to change the pressure in the well, the density will also be modelled as a disturbance. The design choices are listed in table 4.1.

MV	u	Topside choke opening
CV	$\hat{p}_{bit}$	BHP
DV	q_{in}	Main pump flow
	q_{bp}	Back pressure pump flow
	ρ	Mud density

Table 4.1: NMPC variables

In SEPTIC, input blocking is used to reduce calculation time. When input blocking is used, the calculated input is held constant for a time period. And the optimization problem is only solved at certain points of the prediction horizon. Each timestep, where the optimization problem is solved, increases the time needed to calculate the problem. The prediction horizon is set to 500 seconds in all simulations in chapter 5.

Chapter 5

Pressure Control - Simulations and Results

The main result of the simulations will be presented in this chapter. The performance of the NMPC controller will be analyzed, but in order to analyze it, it is convinient to compare it with another controller. In this section the NMPC scheme will be compared against a standard proportional integral (PI) controller. The PI-controller will be given by the following equations:

$$u_k = u_{k-1} + K_p((e_k - e_{k-1}) + \frac{T}{2K_\tau}(e_k + e_{k-1})) \tag{5.1}$$

where

$$e_k = p_{bit,ref} - \hat{p}_{bit} \tag{5.2}$$

and T is the time length of one iteration. K_p and K_τ are controller tuning parameters. The reader may refer to Balcen et al. [2003] for a more thorough introduction to PI-control. It is important to observe that both controllers try to control the estimated pressure. The pressure from the simulator, which will be assumed to be the real pressure in the well, is also plotted, so that the controllers impact on this pressure could be observed.

5.1 WeMod

The well will be simulated with the dynamic well simulator, *WeMod*. *WeMod* is a commercially available software developed by the International Research Institute of Stavanger (IRIS). The user can through a MATLAB interface set the valve opening, the main and annulus pump flow, and the density of the drilling fluid. Based on this values all the pressures and flow characteristics through the well is calculated. A specific pore pressure and permeability can

be given as an input to the simulator, resulting in a dynamic influx from the reservoir. During the following simulations, the influx from the reservoir is turned off. This results in a major simplification of the control problem. As discussed in chapter 1, the influx from the well can contribute to a lower BHP, resulting in a possible kick or an uncontrolled blowout. The interface between SEPTIC and WeMod is written in C++, and at each timestep, the measurements from WeMod is copied to SEPTIC. SEPTIC then optimizes the problem, and calculates a value of the inputs. These inputs are then copied back to WeMod which then simulates one timestep further.

5.2 Parameter Identification

All the parameters in the model and the controller have to be fitted to the simulator. The parameters used are listed in table 5.1. Most of the parameters in the table are taken from Imsland [2007], and some are experimental adjusted to the simulator.

Parameter	Value	Unit
β_a	7000	
β_d	11000	
F_a	15831	
F_d	176640	
G	9.81	$[m/sec]$
H_{bit}	2000	$[m]$
K_ϵ	0.05	
M_a	1621	$[10^{-5}x\frac{kg}{m^4}]$
M_d	6064	$[10^{-5}x\frac{kg}{m^4}]$
M	7685	$[10^{-5}x\frac{kg}{m^4}]$
$P_p(0)$	10	$[bar]$
$q_{bit}(0)$	0.0167	$[m^3/sec]$
ρ_a	0.0125	$[10^(-5)x\frac{kg}{m^3}]$
ρ_d	0.0125	$[10^(-5)x\frac{kg}{m^3}]$
V_a	96.1327	$[m^3]$
V_d	28.2743	$[m^3]$
p_0	183	$[bar]$
K_p	-0.0025	
K_{tau}	15	
C_d	0.0045	

Table 5.1: Parameters used in simulations

5.3 Reference Tracking

The first test scenario is reference tracking. In this scenario, the controllers will be tested on their ability to follow reference variation. Every 500 second the reference is changed by 10 bars. The initial reference on the BHP is 270 bars, and it is increased every 500s until it reaches 320 bars. After reaching this pressure, the reference is decreased at the same speed, until the initial reference at 270 bars is reached. There are no disturbances present in this scenario, since the pump flows are kept steady. The results are presented in figure 5.1 (PI control) and in 5.2 (NMPC).

The figures where the simulations are presented, consist of five different subplots:

1. The valve opening
2. The estimated BHP
3. BHP from the simulator
4. Both the estimated pressure and the BHP from WeMod is plotted together for comparison
5. The ϵ value, which is added to the observer equation

All simulations are carried out with one iteration every second. And at each second the NMPC optimization problem is solved.

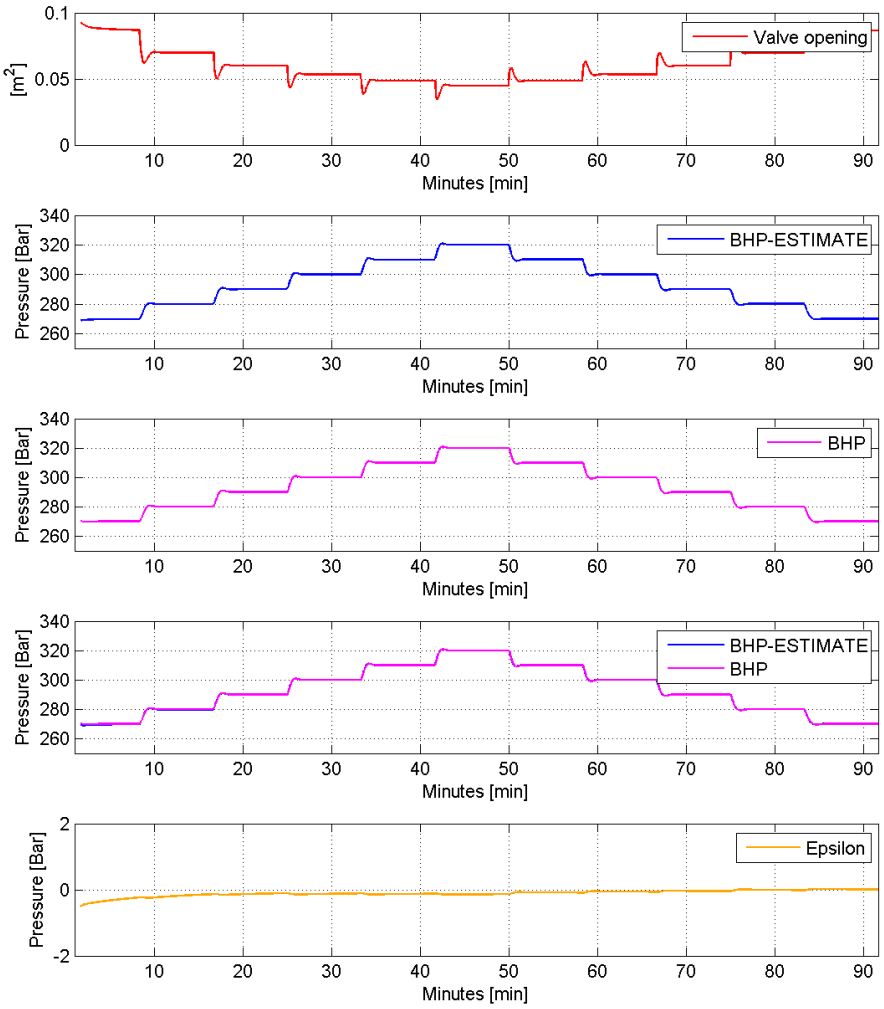

Figure 5.1: Pi control: Reference tracking

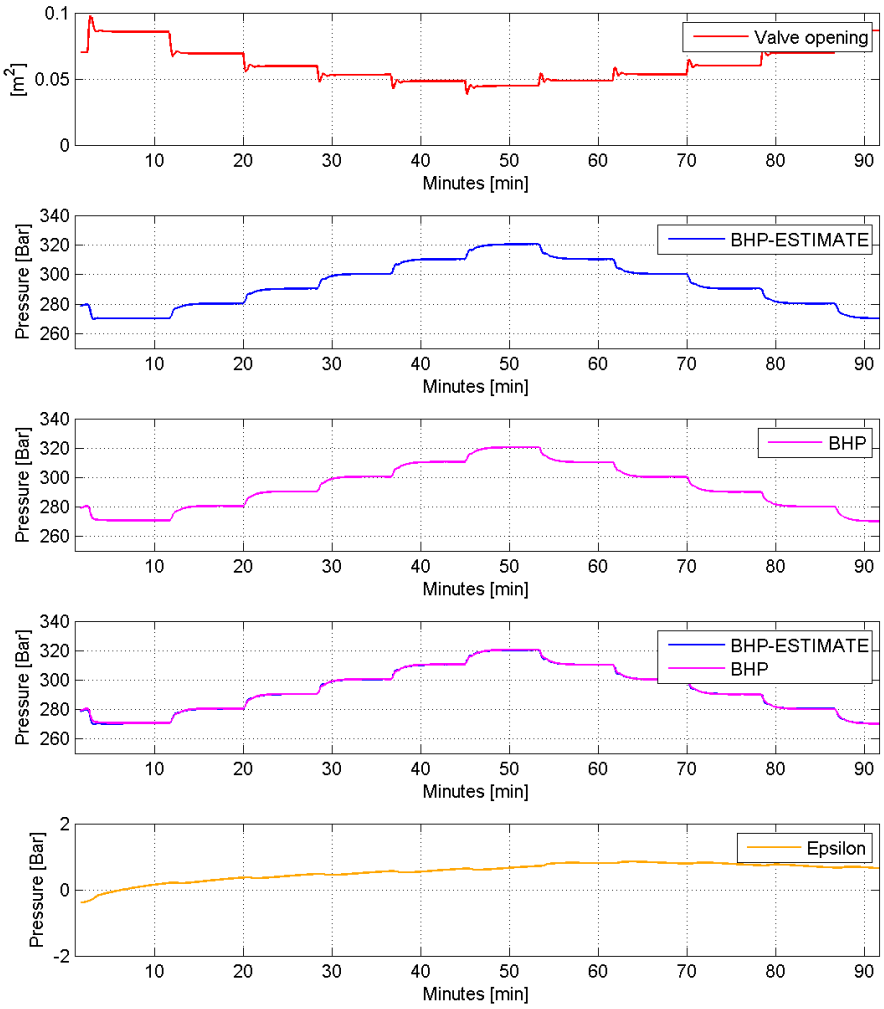

Figure 5.2: NMPC: Reference Tracking

As illustrated in figure 5.1 and 5.2, both the controllers have the ability to track the reference without any problems, when there are no disturbances present. There is one important comment to be made. The PI controller is tuned much tighter then the NMPC controller. The reason for this choice of tuning parameters is not obvious in this scenario, but it is due to the controllers ability to reject disturbances. Since the PI controller has been tuned aggressively, it follows the reference trajectory very well, but it comes with a drawback. The usage of the topside choke is aggressive, and the controller makes the valve overshoot its resting values by a factor of 0.5-6 each time the setpoint is changed. The NMPC controller is not tuned as aggressively as the PI controller, and there is no excessive movement of the valve. There are also a penalty on changing the opening of the choke in the NMPC controller.

5.4 Pipe Connection

If a jointed pipeline is used during drilling, there will be an interruption in the drilling operation each time a new drillpipe is connected. The drillpipe usually consist of pipe segments 100 feet long. During the pipe connection procedure the main pump has to be disconnected, and this will lead to loss of circulation. This procedure is illustrated in figure 5.3. The consequences of lost circulation are variations in the bottomhole pressure, due to reduced friction loss. When circulation is lost, the measurement of the BHP will not be available, since the system is dependent on circulation.[Nygaard, 2006]

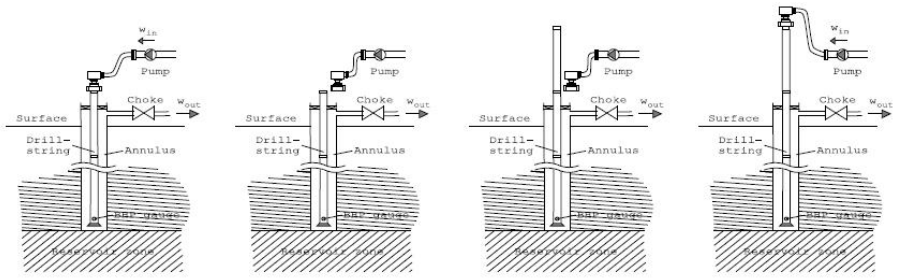

Figure 5.3: Pipe connection procedure[Nygaard, 2006]

To simulate the pipe connection, the annulus pump flow rate is decreased from a flow rate of $1000m^3/min$ to zero flow rate. 30 seconds after the annulus pump reduces its flow, the flow from the backpressure pump is increased from $200m^3/min$ to $400m^3/min$. Figure 5.4 shows the operation of the pumps.

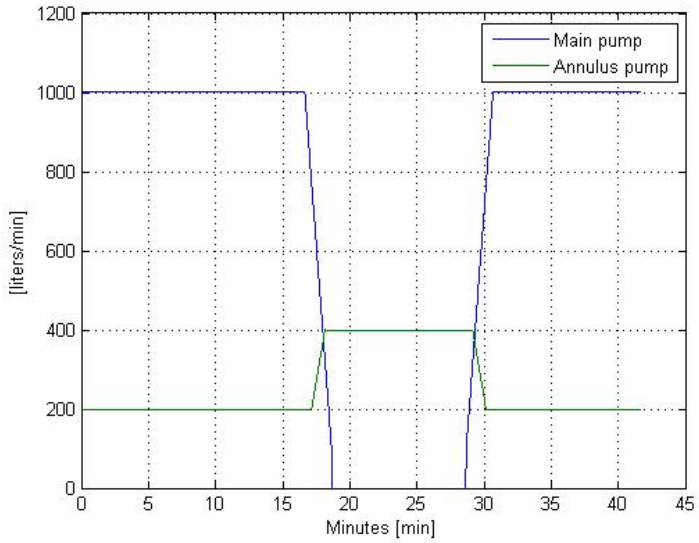

Figure 5.4: Pump flow

The results of the simulations are presented in figure 5.5-5.8. The first two simulations, figure 5.5 and 5.6 are pipe connection procedures with a setpoint of 280 bars. The next two, figure 5.7 and 5.8, are the results of the same scenario, but with a set point of 320 bars.

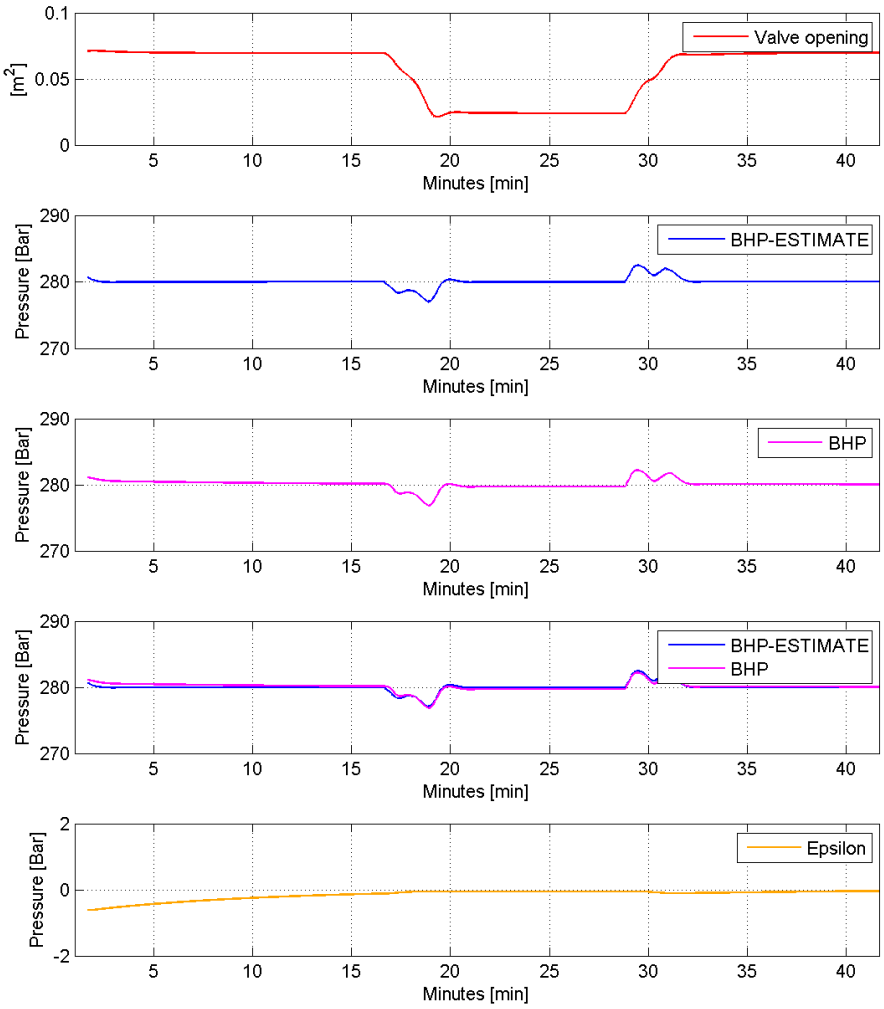

Figure 5.5: PI control: Pipe connection - 280 bar setpoint

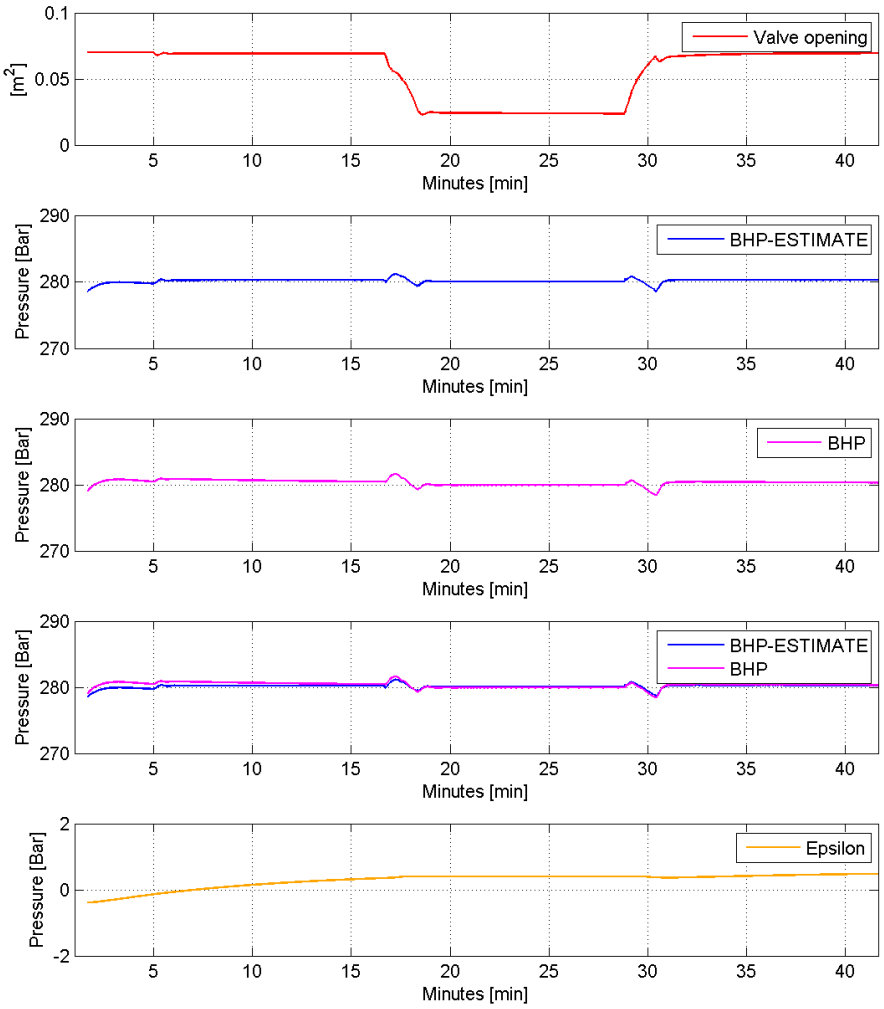

Figure 5.6: NMPC: Pipe connection - 280 bar setpoint

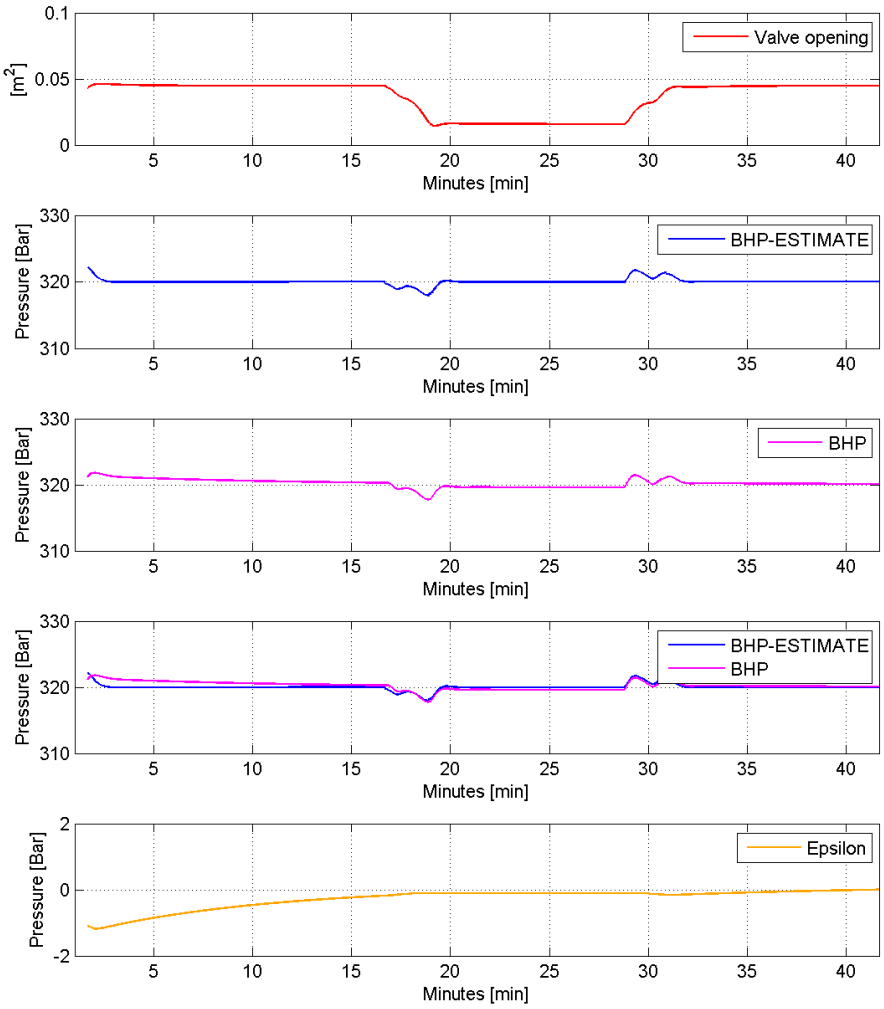

Figure 5.7: Pi control: Pipe Connection - 320 bar setpoint

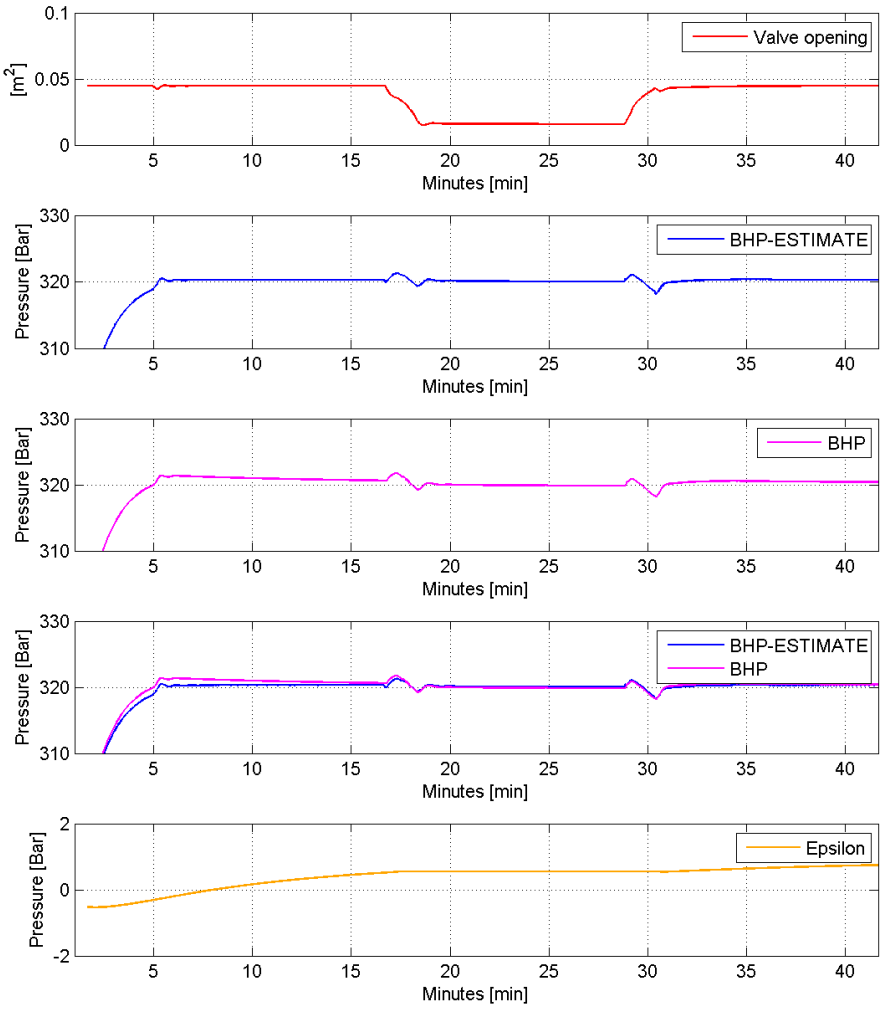

Figure 5.8: NMPC: Pipe connection - 320 bar setpoint

The results show that when the NMPC scheme is used, the BHP is kept within a range of ± 2.0 bars from the setpoint, even though the control is performed on the estimated value and not directly on the BHP. As shown from the simulations with a setpoint of 280 and 320 bars, the performance of the NMPC scheme is indifferent to the value of the setpoint. This is were the NMPC scheme has its strength compared to linear controllers. The performance of a linear controller, such as the PI-controller, will be affected by the variations in setpoint. A PI-controller may be tuned to perform well at one specific pressure, or to one specific scenario, but deviation from this setpoint will reduce the performance of the conroller. In the simulations with PI-control, figure 5.7 and 5.5, it can be seen that the performance of the controller is affected by different setpoint values. The reason why the PI-controller had to be tuned aggressivly is ensure its ability to reject noise. The flow from both pumps are modelled as disturbances, and if the controller were less aggressivly tuned, it would lead to larger variations in the BHP when the flow rates are changed. The maximum deviation from the setpoint when using the PI-controller, is 3 bars. The target of this report has been to maintain the BHP within a range of 2.5 bars from the setpoint, which the PI-controller is not abel to do. When trying to maintain the pressure within these boundaries, it is crucial that the estimated pressure is close to the BHP.

Chapter 6

Conclusion and Future work

6.1 Conclusion

- During drilling operations, large variations in the BHP can be observed. Minimization of these variations is a key factor for the success of the well. Large economical benefits can be the result of a successful well. Managed Pressure Drilling gives the possibility of increased control of the BHP and will in some cases make 'undrillable' wells drillable
- The modifications implemented in the observer has improved the preformance of the obsever. The reduction of the difference between the estimated BHP and the real value of the BHP has proved to be important when trying to control the BHP within narrow constraints.
- An NMPC scheme that fullfills the objective of keeping the BHP within the range of $\pm$ 2.5 bars during a pipe connection procedure has been developed. The performance of the NMPC controllers is indifferent to the operation point compared to a linear PI controller.
- A low order model of the well has turned out to be sufficient to both estimate and control the pressure in the well

6.2 Future work

The model is essential for both the implementation of the observer and the NMPC scheme. The accuracy of the estimation is strongly dependent on the model's ability to describe the fluid mechanics. The flow in a well can under normal conditions consist of liquids, gas and solids, known as a multi-phase flow. The flow patterns in a multi-phase flow are complex, and are not easily described by simple equations, as those used in this report. However, the models have showed to be adequate for both estimating and controlling the BHP when gas is not present in the well. The model should be developed further to take gas into consideration, and to describe the dynamics in the well when a kick occurs. An adequate description will be essential in estimating the BHP, and to be able to handle it by an NMPC scheme.

When using this simplified model to control the pressure in the well, some key parameters should be estimated for control purposes. One important parameter is the compressibility in the annulus, β_a, which will be greatly affected both by gas influx and cuttings. Estimating β_a is crucial for the performance of the controller, while the prediction will be off if the parameter value is wrong.

When drilling into the ground, the temperature increases with increasing depth. The temperature will also be dependent on the temperature of the mud, which can be controlled by mud heaters. The temperature effects in the well has been neglected in the model. The temperature will effect both the density of the mud, and the viscosity. Therefore the temperature effects should be implemented in the model to improve the accuracy. It can also be relevant to control the temperature in the well, to avoid formation of hydrates.

In this report the effects of surge and swab operations (Insertion and extraction of the drillpipe) has not been discussed. Extraction of the drillpipe is one of the main reasons why kicks occur. Controlling the BHP while these operations are carried out, will have great potential for reducing unwanted situations.

Bibliography

Frank Allgöwer, Rolf Findeisen, and Zoltan K. Nagy. Nonlinear model predictive control: From theory to application. *J. Chin. Inst. Chem. Engrs.*, 35:299–315, 2004.

J. J. Azar and G. Robello Samuel. *Drilling Engineering*. PennWell Publishing Company, 2007.

Jens G. Balcen, Trond Andresen, and Bjarne A. Foss. *Reguleringsteknikk*. Institutt for teknisk kybernetikk, 2003.

C. C. Chen and L. Shaw. On receding horizon feedback control. *Automatica*, 18:349–352, 1982.

C. R. Cutler and B. L. Ramaker. Dynamic matrix control - a computer control algorithm. In *AICHE national meeting, Houston, Texas*, 1979.

C. R. Cutler, A. Morshedi, and J. Haydel. An industrial perspective on advanced control. In *AICHE annual meeting, Houston, Texas*, 1983.

Nuno M. C. de Oliveira and Lorenz T. Biegler. An extension of newton-type algoritms for nonlinear process control. *Automatica*, 31:281–286, 1995.

Michael J. Economides, Larry T. Watters, and Shari Dunn-Norman. *Petroleum Well Construction*. John Wiley & Sons, 1998.

Olav Egeland and Jan Tommy Gravdahl. *Modeling and Simulation for Automatic Control*. Marine Cybernetics, 2002.

Michael Golan and Curtis H. Whitson. *Well Performance*. D. Reidel Publishing Company, 1986.

D. Goldfarb and A. Idnani. Numerrically stable dual method for solving strictly convex quadratic programs. *Mathematical Programming*, 27:1–33, 1983.

Robert D. Grace. *Advanced Blowout and Well Control.* Golf Publishing Company, Houston, Texas, 1994.

D. Hannegan. Case studies - offshore managed pressure drilling. In *Proceedings - SPE Annual Technical Conference and Exhibition, ATCE 2006, 1:650-656*, 2006.

Lars Imsland. Mpd estimation. Technical report, SINTEF, 2007.

Ali A. Jalali and Vahid Nadimi. A survey on robust model predictive control from 199-2006. In *International Conference on Computional Intelligence for Modelling Control*, 2006.

Glenn-Ole Kaasa. A simple dynamic model of drilling for control.

R. E. Kalman. Contributions to the theory of optimal control. *Bulletin de la Societe Mathematique de Mexicana*, 5:102–119, 1960a.

R. E. Kalman. A new approach to linear filtering and prediction problems. *Transactions of ASME, Journal of Basic Engineering*, 87:35–45, 1960b.

L. Magni and R. Sepulchre. Stability margins of nonlinear receding-horizon control via inverse optimality. *Systems & Control Letters*, 32:241–245, 1997.

D. Q. Mayne and H. Michalska. Receding horizon control of nonlinear systems. *Automatica*, 35:814, 1990.

D. Q. Mayne, James B. Rawlings, C. V. Rao, and P. O. M. Scokaert. Constrainted model predicitve control: Stability and optimality. *Automatica*, 36:789–814, 2000.

Patrick Meum. Optimal reservoir control using nonlinear mpc and eclipse. Master's thesis, Norwegian University of Science and Technology (NTNU), 2007.

H. Michalska and D. Q. Mayne. Robust receding horizon control of constrained nonlinear systems. *IEEE Transactions on Automatic Control*, 38: 1623–1633, 1993.

Preston L. Moore. *Drilling Practices Manual.* PennWell Publishing Company, 1986.

Bruce R. Munson, Donald F. Young, and Theodore H. Okiishi. *Fundamentals of Fluid Mechanics.* Van Hoffmann Pres Inc., 1998.

J. Nocedal and S. J. Wright. *Numerical Optimization*. Springer, 1999.

Gerhard H. Nygaard. *Multivariable process control in high temperature and high pressure environment using non-intrusive multi sensor data fusion*. PhD thesis, Norwegian University of Science and Technology, 2006.

Gerhard H. Nygaard and Geir Nævdal. Nonlinear model predicitve control scheme for stabilizing annulus pressure during oil well drilling. *Journal of Process Control*, 16:719–732, 2006.

Gerhard H. Nygaard, Geir Nævdal, and Saba Mylvaganam. Evaluating nonlinear kalman filters for parameter estimation in reservoirs during petroleum well drilling. In *International Conference on Control Applications*, 2006.

Gerhard H. Nygaard, Erlend H. Vefring, Kjell-Kåre Fjelde, Geir Nævdal, Rolf Johan Lorentzen, and Saba Mylvaganam. Bottomhole pressure control during drilling operations in gas-dominant wells. *SPE Journal*, March:49–61, 2007.

S. Joe Qin and Thomas A. Badgwell. A survey of industrial model predicitve control technology. *Control Engineering Practice*, 11:733–764, 2003.

James B. Rawlings. Tutorial overview of model predictive control. *IEEE Control Systems Magazine*, 20:38–52, 2000.

J. Richalet, A. Rault, J. L. Testud, and J. Papon. Algorithmic control of industrial processes. In *Proceedings of the 4th IFAC symposium on identification and system parameter estimation. 1119-1167*, 1976.

J. Richalet, A. Rault, J. L. Testud, and J. Papon. Model predictive heuristic control: Applications to industrial processes. *Automatica*, 14:413–428, 1978.

Thomas Rognmo. Performance and robustness-analysis of mpd control. Technical report, Norwegian University of Science and Technology (NTNU), 2007.

K. Schittkowski. Ql: A fortran code for convex quadratic programming. Technical report, University of Bayreuth, 2005.

P. O. M. Scokaert, J.B. Rawlings, and E. S. Meadows. Discrete-time stability with pertubations: Application to model predictive control. *Automatica*, 33:463–470, 1997.

Dulce C. M. Silva and Nuno M. C. Oliveira. Optimization and nonlinear model predicitve control of batch polymerization systems. *Computers and Chemical Engineering*, 26:649–658, 2002.

Pål Skalle. *Pressure control during drilling.* Tapir Akademiske Forlag, 2005.

Sigurd Skogestad and Ian. Postlethwaite. *Multivariable Feedback Control.* John Wiley & Sons, 2005.

Stig Strand and Jan Richard Sagli. Mpc in statoil - advantages with in-house technology. *Proc. ADCHEM*, pages 97–103, 2003.

Yaolong Tan, Ioannis Kanellakopoulos, and Zhong-Ping Jiang. Nonlinear observer/controller design for a class of nonlinear systems. In *Proceedings of the 37th IEEE Conference on Decision & Control*, 1998.

Håvard Torpe. Pipeline liquid control using nonlinear mpc and olga. Master's thesis, Norwegian University of Science and Technology, Department of Engineering Cybernetics, 2007.

Frank M. White. *Fluid Mechanics, 5th edition.* 2003.

C. Yousfi and R. Tournier. Steady state optimization inside model predictive control. In *Proceedings of the American Control Conference, 2: 1866-1870*, 1991.

Øyvind Nistad Stamnes. Adaptive observer for bottomhole pressure during drilling. Master's thesis, NTNU - Norwegian University of Science and Technology, 2007.

Alex Zheng and Manfred Morari. Stability of model predictive control with mixed constraints. *IEEE Transactions on automatic control*, 40:1818–1823, 1995.

Appendix A

Variables in the NMPC Application

```
  Cvr:           BHP_STAMNES_ESTIMATE
 Text1=  ""
 Text2=  ""
  Mode=  ACTIVE
  Auto=  OFF
   PlotMax=  400
   PlotMin=  200
  PlotSpan=  -1
   PlotGrp=  00000000000000000000000000001000
XvrMnu=  0000000000000000
  Nfix=  3
MaxChg=  -1
  Unit=  "Bar"
  Meas=  300
   GrpMask=  00000000000000000000000000000001
   GrpType=  00000000000000000000000000000000
  Span=  50
  SetPntOn=  280
HighOn=  285
 LowOn=  275
SetPntPrio=  2
  HighPrio=  1
   LowPrio=  1
  Fulf=  200
 HighPnlty=  20
  LowPnlty=  1000
 HighLimit=  1000
```

```
  LowLimit=  1000
 RelxParam=  4    1   30   80   150
   FulfReScale=  0.001
  SetpTref=  1
 BiasTfilt=  0
 BiasTpred=  0
 ConsTfilt=  -1
 Integ=  0
 TransformType=  NOTRANS
 BadCntLim=  0
   DesHorz=  0
 Neval=  5
EvalDT=  0
   KeepTargets=  OFF

     Mvr:           CVALVE
 Text1=  ""
 Text2=  ""
  Mode=  TRACKING
  Auto=  OFF
   PlotMax=  1.4
   PlotMin=  0
  PlotSpan=  -1
   PlotGrp=  00000000000000000000000000000010
XvrMnu=  0000000000000000
  Nfix=  4
MaxChg=  -0.01
  Unit=  "%"
  Meas=  1
   GrpMask=  00000000000000000000000000000001
   GrpType=  00000000000000000000000000000000
  Span=  0.05
HighOn=  0.1
 LowOn=  0.00001
ProcessValueBAD=  0
 IvOff=  0
 MaxUp=  1
 MaxDn=  -1
 MovePnlty=  100
 IvRoc=  -1
IvPrio=  99
  Fulf=  1
   FulfReScale=  0.1
```

```
 Price=  0
  Blocking=  9    2    4    7   11   16   22 50 100 200

     Dvr:           MAIN_PUMP_FLOW
 Text1=  ""
 Text2=  ""
  Mode=  TRACKING
   PlotMax=  1000
   PlotMin=  0
  PlotSpan=  -1
   PlotGrp=  00000000000000000000000000000001
XvrMnu=  0000000000000000
  Nfix=  3
  Unit=  "kg/s"
  Meas=  1000
   GrpMask=  00000000000000000000000000000001
   GrpType=  00000000000000000000000000000000
  Span=  300

  Dvr:           ANNULUS_PUMP_FLOW
 Text1=  ""
 Text2=  ""
  Mode=  TRACKING
   PlotMax=  500
   PlotMin=  0
  PlotSpan=  -1
   PlotGrp=  00000000000000000000000000000001
XvrMnu=  0000000000000000
  Nfix=  3
  Unit=  "kg/s"
  Meas=  200
   GrpMask=  00000000000000000000000000000001
   GrpType=  00000000000000000000000000000000
  Span=  100

Dvr:          Density
 Text1=  ""
 Text2=  ""
  Mode=  TRACKING
   PlotMax=  0.04
   PlotMin=  0.01
  PlotSpan=  -1
   PlotGrp=  00000000000000000000000000000001
```

```
XvrMnu=  0000000000000000
  Nfix=  3
  Unit=  "kg/s"
  Meas=  0.0125
   GrpMask=  00000000000000000000000000000001
   GrpType=  00000000000000000000000000000000
  Span=  0.01
```

Appendix B

Derivation of the Equation of Continuity

An elemental control volume in carthesian coordinates are used to derive the basic differential equation. The elemental control volume is infinitesimal and it is illustrated in figure B.1. There is a flow through all six faces of the control volume, which are approximated to be one-dimensional. The differential equation for the control volume will be

$$\int_{CV} \frac{\partial \rho}{\partial t} dV + \sum m_{out} - \sum m_{in} = 0 \tag{B.1}$$

The volume integral can be approximated to the differential term, since the elemental volume is so small:

$$\int_{CV} \frac{\partial \rho}{\partial t} dV \approx \frac{\partial \rho}{\partial t} dxdydz \tag{B.2}$$

If the inflow through the right surface of the conrol volume is assumed to be equal to ρu, then the outflow will be $\rho u + \frac{\partial}{\partial x}(\rho u)dx$. This is the situation illustrated in figure B.1. The flow through all the six surfaces are listed in table B.1. The equations in table B.1 is inserted into equation B.1

Table B.1: 3-Dimensional Flow[White, 2003]

Face	Inlet mass flow	Outlet mass flow
x	$\rho u dydz$	$(\rho u + \frac{\partial}{\partial x}(\rho u)dx)dydz$
y	$\rho v dydz$	$(\rho v + \frac{\partial}{\partial y}(\rho v)dy)dxdz$
z	$\rho w dydz$	$(\rho w + \frac{\partial}{\partial w}(\rho w)dz)dxdy$

$$\frac{\partial \rho}{\partial t} dxdydz + \frac{\partial}{\partial x}(\rho u)dxdydz + \frac{\partial}{\partial y}(\rho v)dxdy + \frac{\partial}{\partial z}(\rho w)dxdydz \tag{B.3}$$

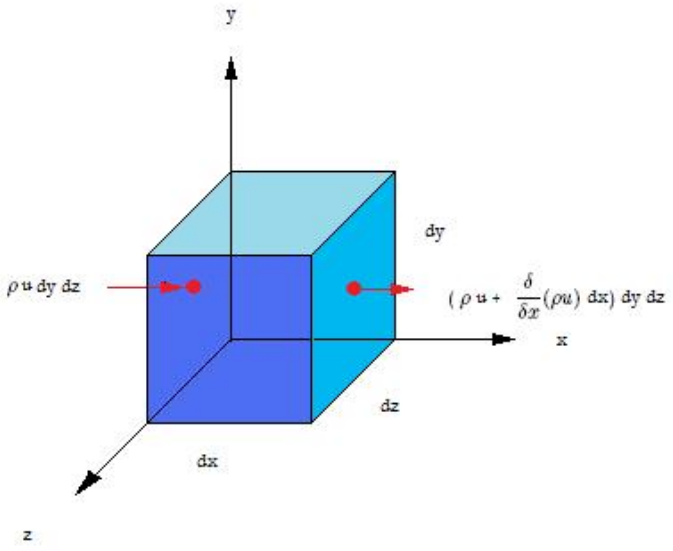

Figure B.1: Elemental Control Volume

Cancel out the element volumes.

$$\frac{\partial \rho}{\partial t} + \frac{\partial}{\partial x}(\rho u) + \frac{\partial}{\partial y}(\rho v) + \frac{\partial}{\partial z}(\rho w) = 0 \tag{B.4}$$

This is often referred to as the *equation of continuity* because it requires no assumptions except that of density and velocity as continuum functions. The latter states that the flow may be either steady or unsteady, viscous or frictionless, compressible or incompressible [White, 2003]. This result will also be used in chapter C, when deriving the equation of motion. For the well an assumption of one dimensional flow in the x-direction (vertical flow) will be made. This assumption reduces the full continuity equation to a one-dimensional expression.

$$\frac{\partial \rho}{\partial t} + \frac{\partial}{\partial x}(\rho u) = 0 \tag{B.5}$$

Appendix C

Derivation of the Equation of Momentum

In this chapter linear momentum will be discussed. Newtons second law of motion is used in conjunction with the approach from section 2.3. An infinitesimal elemental volume, using the linear momentum relation

$$\sum F = \frac{\partial}{\partial t}(\int_{CV} V_s \rho \text{ dV}) + \sum (\dot{m} V_s)_{out} + \sum (\dot{m} V_s)_{in} \tag{C.1}$$

will be considered. V_s is a vector describing the speed of the fluid in carthesian coordinates, V_s = [u v w]. Again the volume integral, due to it's small volume, can be approximated to

$$\frac{\partial}{\partial t}(V_s \rho \text{ dV}) \approx \frac{\partial}{\partial t}(\rho V_s) \text{ dx dy dz} \tag{C.2}$$

The momentum flux occurs on all six surfaces of the elemental volume, and the size of the flux on each surface can be found in table C.1.

Table C.1: Momentum Flux[White, 2003]

Face	Inlet Momentum Flux	Outlet Momentum Flux
x	ρu V$_s$ dy dz	$(\rho u$ V$_s + \frac{\partial}{\partial x}(\rho u$ V$_s)$ dx) dy dz
y	ρv V$_s$ dy dz	$(\rho v$ V$_s + \frac{\partial}{\partial y}(\rho v$ V$_s)$ dy) dx dz
z	ρw V$_s$ dy dz	$(\rho w$ V$_s + \frac{\partial}{\partial w}(\rho w$ V$_s)$ dz) dx dy

These terms are inserted into equation 2.30 resulting in

$$\sum F = dxdydz \left[\frac{\partial}{\partial t}(\rho V_s) + \frac{\partial}{\partial x}(\rho u V_s) + \frac{\partial}{\partial y}(\rho v V_s) + \frac{\partial}{\partial z}(\rho w V_s)\right] \tag{C.3}$$

Using the method described in White [2003] and splitting the terms in the bracket gives:

$$\sum F = dxdydz \left[\frac{\partial \rho}{\partial t} + V_s(\frac{\partial}{\partial x}(\rho u) + \frac{\partial}{\partial y}(\rho v) + \frac{\partial}{\partial z}(\rho w)) \right.$$
$$\left. +\rho(\frac{\partial V_s}{\partial t} + u\frac{\partial V_s}{\partial x} + v\frac{\partial V_s}{\partial y} + w\frac{\partial V_s}{\partial z}) \right] \tag{C.4}$$

The left part of the equation is the continuity equation (Derived in chapter 2.3, equation B.4), which is equal to zero. The resulting part of the equation is therefore:

$$\sum F = dxdydz \left[\rho(\frac{\partial V_s}{\partial t} + u\frac{\partial V_s}{\partial x} + v\frac{\partial V_s}{\partial y} + w\frac{\partial V_s}{\partial z}) \right] = \rho\frac{dV_s}{dt}dxdydz \tag{C.5}$$

If the assumption of a one dimensional vertical flow is used, the resulting equation will be:

$$\sum F = \rho\frac{dV_s}{dt}A(x)dx \tag{C.6}$$